Reassessment of modeling turbulence via Reynolds averaging

A review of second-moment transport strategy

Hanjalić, K.; Launder, B. E.

Important note
To cite this publication, please use the final published version (if applicable).
Please check the document version above.

Reassessment of modeling turbulence via Reynolds averaging: A review of second-moment transport strategy

K. Hanjalić and B. E. Launder

COLLECTIONS

Paper published as part of the special topic on Tribute to Frank M. White on his 88th Anniversary

View Online   Export Citation   CrossMark

ARTICLES YOU MAY BE INTERESTED IN

On closures for reduced order models—A spectrum of first-principle to machine-learned avenues
Physics of Fluids **33**, 091301 (2021); https://doi.org/10.1063/5.0061577

On generalist scholarship: A hierarchical view of research
Physics of Fluids **33**, 091401 (2021); https://doi.org/10.1063/5.0063899

Special topic on turbulent and multiphase flows
Physics of Fluids **33**, 090401 (2021); https://doi.org/10.1063/5.0066618

Reassessment of modeling turbulence via Reynolds averaging: A review of second-moment transport strategy

K. Hanjalić[1,a)] (iD) and B. E. Launder[2,b)] (iD)

AFFILIATIONS

[1]Faculty of Applied Sciences, Delft University of Technology, Delft 2629 HZ, The Netherlands
[2]School of Mechanical, Aerospace & Civil Engineering, University of Manchester, Manchester M1 9PL, United Kingdom

Note: This paper is part of the special topic, Tribute to Frank M. White on his 88th Anniversary.
[a)]khanjalic@gmail.com
[b)]Author to whom correspondence should be addressed: brian.launder@manchester.ac.uk

ABSTRACT

This paper examines the evolution of closing the Reynolds-averaged Navier–Stokes equations by approximating the Reynolds stresses via the second-moment transport equations themselves. This strategy first proposed by Rotta is markedly in contrast to the more usual approach of computing an effective "turbulent viscosity" to deduce the turbulent stresses as in a Newtonian fluid in laminar motion. This paper covers the main elements in the development of this approach and shows examples of applications in complex shear flows that collectively include the effects of three-dimensional straining, force fields, and time dependence that affect the flow evolution in ways that cannot be readily mimicked with an eddy viscosity model.

Published under an exclusive license by AIP Publishing. https://doi.org/10.1063/5.0065211

I. INTRODUCTION

This review summarizes proposals for closing the Reynolds equations for a fluid in turbulent motion by the strategy commonly referred to as *stress-transport modeling*. The writers adopt the more general term "second-moment closure" so as to include cases where convective heat or species transport is either itself the main focus of attention or where they affect the dynamic flow field. While no attempt is made to go into all the details of any model, we do, however, try to provide some explanation of why the subject evolved in the way that it did and give an impression of the roles played by some of the major contributors to the subject. Thus, unlike a typical research paper in turbulence modeling, the authors hope that the contents will be readable and, indeed, read by many whose own research interest lies in quite different areas of Computational Fluid Dynamics (CFD) or whose interest in the physics of turbulence is unconnected with CFD.

This review does not venture into the field of turbulence modeling of combustion or of two-phase flows; nor of high-Mach-number or compressible flows. These important omissions were mandated partly to keep the paper to a manageable length and partly to acknowledge that these are not areas to which we have personally contributed.

Nevertheless, there seems no reason to suppose that the striking improvements from adopting second-moment closures presented below will not carry over to situations where density gradients are vastly greater than those considered here, particularly if density-weighted averaging is adopted. To the areas which *are* covered, the authors bring not only their knowledge but also their prejudices to this account. Thus, the reader should recognize that our choice of key proposals and publications is a personal one that may differ in at least some respects from what others attempting a correspondingly brief overview would have selected.

We start from the unsteady short-term-averaged form of the equations of motion first introduced by Osborne Reynolds, commonly known as the Reynolds equation.[1] For most of Reynolds' paper he adopted a variable density approach that would have taken him to what is nowadays termed Favre averaging.[2] However, he limited further analysis to attempting to show why water (considered a uniform density fluid) flowing through a plane channel underwent transition from laminar to turbulent at a particular value of the dimensionless group we call the Reynolds number. The equation may be written

$$\frac{\partial U_i}{\partial t} + \frac{\partial U_j U_i}{\partial x_j} = \sum_n F_i^n - \frac{1}{\rho}\frac{\partial P}{\partial x_i} + \frac{\partial}{\partial x_j}\left[\nu\left(\frac{\partial U_i}{\partial x_j} + \frac{\partial U_j}{\partial x_i}\right) - \overline{u_i u_j}\right].$$

(1)

Here, independent variables t and x_j track time and space variations in the mean velocity U_i and pressure P; F_i^n are source-like contributions from body forces (of which there may be more than one); and ρ and ν are the fluid density and kinematic viscosity. Finally, the second-order tensor $\overline{u_i u_j}$ is the kinematic *Reynolds stress* that has arisen from averaging the non-linear convection term in the Navier–Stokes equations. It is an unknown quantity and the subject of *turbulence modeling* has, to a large extent, been, about devising a path for its determination.

Boussinesq[3] had suggested, even prior to Reynolds' paper, that turbulent flow should be treated in the same way as a laminar flow but with a much larger effective turbulent viscosity,

$$\overline{u_i u_j} = -\nu_t\left(\frac{\partial U_i}{\partial x_j} + \frac{\partial U_j}{\partial x_i}\right).$$

(2)

Thus, the task of determining a second-order tensor was reduced to that of determining the turbulent viscosity, presumed to be a scalar quantity. Although their analyses had not explicitly adopted an eddy-viscosity assumption, Taylor[4] and Prandtl,[5] examining the consequences in a simple shear flow of an eddy being displaced in the direction of the velocity gradient, arrived at forms that did imply a turbulent viscosity: the *mixing-length hypothesis* was born! In the years that followed, other far more elaborate if incomplete routes to modeling turbulence were put forward. However, with the arrival of the 1960s and the digital computer with its scope for solving numerically the Reynolds equations (at least for relatively simple cases), the principal focus of attention of engineering turbulence-modeling research was once again focused on modeling based on Eq. (2).

Over the rather more than half a century that this class of models has been used in CFD codes, both in research establishments and industry, many successful computations have been made. However, there must have been nearly as many cases, especially in separated flows or where force fields exert a strong effect on the turbulence structure, where the predictions either seriously fail to capture some important aspects of the flow or where the level of accuracy falls short of that desired.

The response of the CFD community to these shortcomings has principally been to turn to a more detailed approach to modeling turbulence: large-eddy simulation (LES) or some less demanding hybrid of LES and Reynolds-averaged Navier–Stokes (RANS) modeling such as Detached-eddy Simulation.[6] While such innovations are to be welcomed and provide a valuable addition to the turbulence-modeling arsenal, the writers' belief, developed over the remainder of this paper, is that many of the shortcomings of widely used turbulence modeling approaches stem from the use of Eq. (2) rather than an inherent inadequacy of Reynolds averaging.

II. DEVELOPMENT OF SECOND-MOMENT CLOSURE

The first explicit proposal that, to determine the Reynolds stresses, one should approximate and then solve the exact but unclosed equation for $\overline{u_i u_j}$ was made by Rotta.[7] The exact equation is obtained by taking moments of the Navier–Stokes equations weighted by the turbulent velocity, u_i or u_j and averaging the result,

$$\underbrace{\frac{\partial \overline{u_i u_j}}{\partial t}}_{\mathcal{L}_{ij}} + \underbrace{U_k \frac{\partial \overline{u_i u_j}}{\partial x_k}}_{\mathcal{C}_{ij}}$$

$$= -\underbrace{\left(\overline{u_i u_k}\frac{\partial U_j}{\partial x_k} + \overline{u_j u_k}\frac{\partial U_i}{\partial x_k}\right)}_{\mathcal{P}_{ij}} + \underbrace{\frac{1}{\rho}\sum_n\left(\overline{f_i^n u_j} + \overline{f_j^n u_i}\right)}_{\mathcal{F}_{ij}}$$

$$+ \underbrace{\frac{1}{\rho}\overline{p\left(\frac{\partial u_i}{\partial x_j} + \frac{\partial u_j}{\partial x_i}\right)}}_{\Phi_{ij}} - \underbrace{2\nu\overline{\frac{\partial u_i}{\partial x_k}\frac{\partial u_j}{\partial x_k}}}_{\varepsilon_{ij}}$$

$$+ \underbrace{\frac{\partial}{\partial x_k}\left[\nu\frac{\partial \overline{u_i u_j}}{\partial x_k} - \overline{u_i u_j u_k} - \frac{1}{\rho}\left(\overline{pu_i}\delta_{jk} + \overline{pu_j}\delta_{ik}\right)\right]}_{\mathcal{D}_{ij}^\nu + \mathcal{D}_{ij}^t + \mathcal{D}_{ij}^p}.$$

(3)

The first terms on the right side of the equation show the direct generation of the turbulent stresses by mean velocity gradients and force fields, the f_i denoting the fluctuating body force linked to turbulence. Note that at this level of modeling $\mathcal{P}_{ij}$ requires no approximation in a complete second-moment closure; nor, in many cases, will $\mathcal{F}_{ij}$. Indeed, much may be learned about the qualitative response of turbulence to different types of strain and force fields just from examining those terms. As just a single, frequently cited example, consideration of the additional elements of $\mathcal{P}_{ij}$ active in boundary layers developing on a curved surface explains why the flow is so extraordinarily sensitive to the extra straining that the surface curvature imposes. For then, in a two-dimensional boundary layer (where subscript 1 denotes the primary flow direction and 2 the direction of primary velocity gradient) the generation rate of shear stress, $\overline{u_1 u_2}$, is just

$$\mathcal{P}_{12} = -\left(\overline{u_2^2}\frac{\partial U_1}{\partial x_2} + \overline{u_1^2}\frac{\partial U_2}{\partial x_1}\right).$$

The first term on the right contains the primary velocity gradient while the second is the curvature strain that will be at least an order of magnitude smaller than the primary term. Nevertheless, because the streamwise normal stress, $\overline{u_1^2}$, becomes an order of magnitude greater (and more) than $\overline{u_2^2}$ as the wall is approached, the curvature contribution has an unexpectedly large effect. (Further illustrations of the insight that examining the generation terms provides appear, for example, in Hanjalic and Launder[8]). By contrast, with an eddy-viscosity model, as is evident from the form of Eq. (2), any extra sensitivity to streamline curvature has to be added empirically, and then one will usually discover that a correction designed for one type of curvature is not at all suitable for another!

Of course, one cannot escape from the task of modeling, the unknown terms, here represented by the short-hand symbols Φ_{ij}, ε_{ij}, $\mathcal{D}_{ij}^t$, and $\mathcal{D}_{ij}^p$. It is worth noting that Rotta[7] advocated this level of closure not as a refinement to but as a *simplification of* proposals then in vogue. Millionshtchikov[9] had argued that the fourth-order products, $\overline{u_i u_j u_k u_l}$ (which appear as unknowns in the triple-product transport equations, i.e., for $\overline{u_i u_j u_k}$) could be reliably approximated in terms of products of the Reynolds stresses. Thus, workers at the time, e.g., Chou,[10] had suggested third-moment closure as the logical level at which to close the equation set. In fact, third-moment closure, even when computer capacity and speed had grown sufficiently to make

such an approach feasible, has not attracted a significant following apart from a few papers on horizontal shear flows strongly damped by gravitational forces (André et al.[11] and Craft et al.[12]). Thus, today it is widely accepted that second-moment closure is the highest level of RANS modeling worth adopting for general application.

Rotta[7] was the first to bring out clearly that the crucially important pressure-strain correlation, Φ_{ij}, should have distinct contributions from both the turbulence field, Φ_{ij1} (sometimes called the "slow" part) and the mean strain, Φ_{ij2} (termed the "rapid" part). His proposal for the former is still retained in many models to this day,

$$\Phi_{ij1} = -c_1\left[\overline{u_iu_j} - 2/3\delta_{ij}k\right]/\mathcal{T}, \qquad (4)$$

where k is the turbulence energy, $\overline{u_ku_k}/2$. The proposal indicates that the term tends to drive turbulence back toward its isotropic state, $\overline{u_iu_j} = 2/3\delta_{ij}k$, as is observed to occur in the absence of mean strain. The timescale $\mathcal{T}$ is usually taken as k/ε where ε is the viscous dissipation rate of k with the coefficient c_1 taken as constant. In fact, some of the early closure proposals retained just Eq. (4) as the complete model of Φ_{ij}. While Rotta had made outline suggestions for the mean-strain contribution to Φ_{ij}, the first tensor-based proposal was by Naot et al.,[13] essentially applying a similar return-to-isotropy idea as Eq. (4),

$$\Phi_{ij2} = -c_2\left[\mathcal{P}_{ij} - 1/3\delta_{ij}\mathcal{P}_{kk}\right]. \qquad (5a)$$

This approximation is known as the "Isotropization of Production," IP model. If one adopts a rotating reference frame to examine a spinning flow, a further quasi-production term, $\mathcal{R}_{ij}$, appears in Eq. (3) associated with the axis rotation: $\mathcal{R}_{ij} = -2\Omega_k\left[\overline{u_ju_m}\epsilon_{ikm} + \overline{u_iu_m}\epsilon_{jkm}\right]$ where Ω_k is the angular rotation rate about axis x_k and ϵ_{ikm} is the third rank alternating unit tensor. However, in order to make the conventional convection tensor frame indifferent, it needs to receive half of this rotational "generation." Thus, the appropriate form of Eq. (5a) for such rotating systems should be:

$$\Phi_{ij2} = -c_2\left[\mathcal{P}_{ij} + 1/2\mathcal{R}_{ij} - 1/3\delta_{ij}\mathcal{P}_{kk}\right]. \qquad (5b)$$

The body-force analog of Eq. (5) has been proposed and successfully applied to buoyant generation by Launder[14] and magnetic effects by Schumann[15] and Kenjeres et al.[16] as will be exemplified in considering stratified flows below. There was initially a wide range of values proposed for the two empirical coefficients, c_1 and c_2. However, in local equilibrium where generation and dissipation rates of k are in balance, it is readily shown that there is really just a single parameter $(1 - c_2)/c_1$ and, as we see from Fig. 1, all proposals lie close to the line $c_1 = (1 - c_2)/0.23$. Thus, for applications close to local equilibrium undergoing simple shearing, similar results would be given by all the models named in Fig. 1. Rapid-Distortion Theory (that assumes viscous dissipation to be negligible) applied to isotropic turbulence[17] leads to a result that also agrees with Eq. (5) provided the coefficient c_2 is chosen as 0.6; in that case, c_1 takes a value of approximately 1.7. Values close to these are commonly adopted in models using this formulation today.

A powerful early application of this "basic" model of Φ_{ij} is shown in Fig. 2 relating to the flow through an annular diffuser of a gas turbine computed by Jones and Manners.[18] Of the remaining terms in Eq. (3) to be modeled, they took the dissipation processes, ε_{ij}, to be isotropic, i.e.,
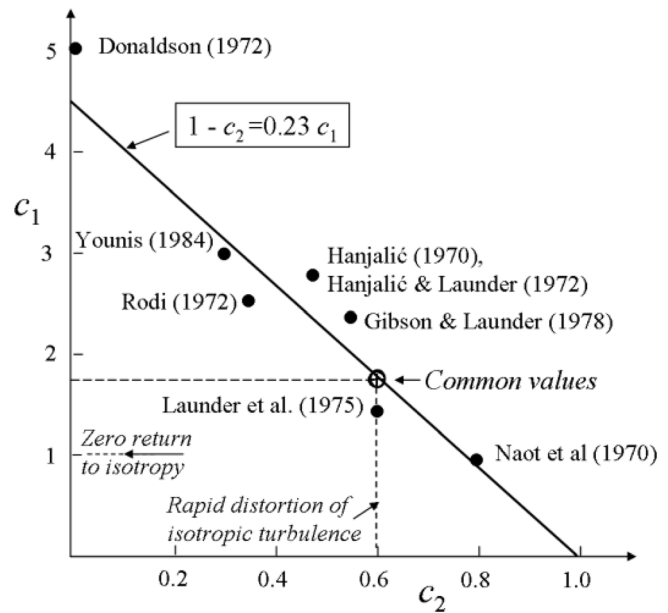

FIG. 1. Map of proposals for coefficients in the Basic Model for Φ_{ij}, Eqs. (4) and (5). Reproduced with permission from K. Hanjalić and B. E. Launder, *Modeling Turbulence in Engineering and the Environment* p. 69 (2011). Copyright 2011, Cambridge University Press.

$$\varepsilon_{ij} = 2/3\delta_{ij}\varepsilon, \qquad (6)$$

where ε is the viscous dissipation rate (whose modeling is discussed later) and made simple gradient-diffusion assumptions for the non-critical diffusion processes. Evidently, the eddy-viscosity model (EVM) fails to capture the impact on the turbulent shear stress of the streamline curvature due to the bends following the inlet and just before the exit. Consequently, the predicted velocity distribution (at entry to the combustion chamber) is of quite the wrong shape – indeed, worse than just assuming a uniform inlet velocity distribution! The second-moment model, however, closely mimics the experimental data.

In one of the earliest applications of second-moment closure to an inhomogeneous flow, the present writers considered the strongly asymmetric flow through a plane channel, the asymmetry being caused by roughening one of the walls.[20] Industry's interest in such a basic flow sprang from the suspicion that in strongly asymmetric flows the position of zero shear stress would not coincide with the position of maximum velocity. The experiments, indeed, fully confirmed that the shear stress vanished closer to the smooth surface than the velocity maximum and that the minimum k lay still closer to the smooth wall. Moreover, as seen in Fig. 3, these features were all accurately reproduced by the subsequent computations.[21]

In this case, the diffusional transport of the Reynolds stresses was very important since the separation between the location of peak velocity and zero shear stress may be unambiguously attributed to that process. A popular scheme for modeling diffusive transport at the second-moment level is known as the *generalized gradient-diffusion hypothesis* (GGDH) originally adopted by Daly and Harlow,[22]

$$\mathcal{D}_\varphi = \frac{\partial}{\partial x_k}\left[c_\varphi \frac{k\overline{u_ku_l}}{\varepsilon}\frac{\partial\varphi}{\partial x_l}\right], \qquad (7)$$
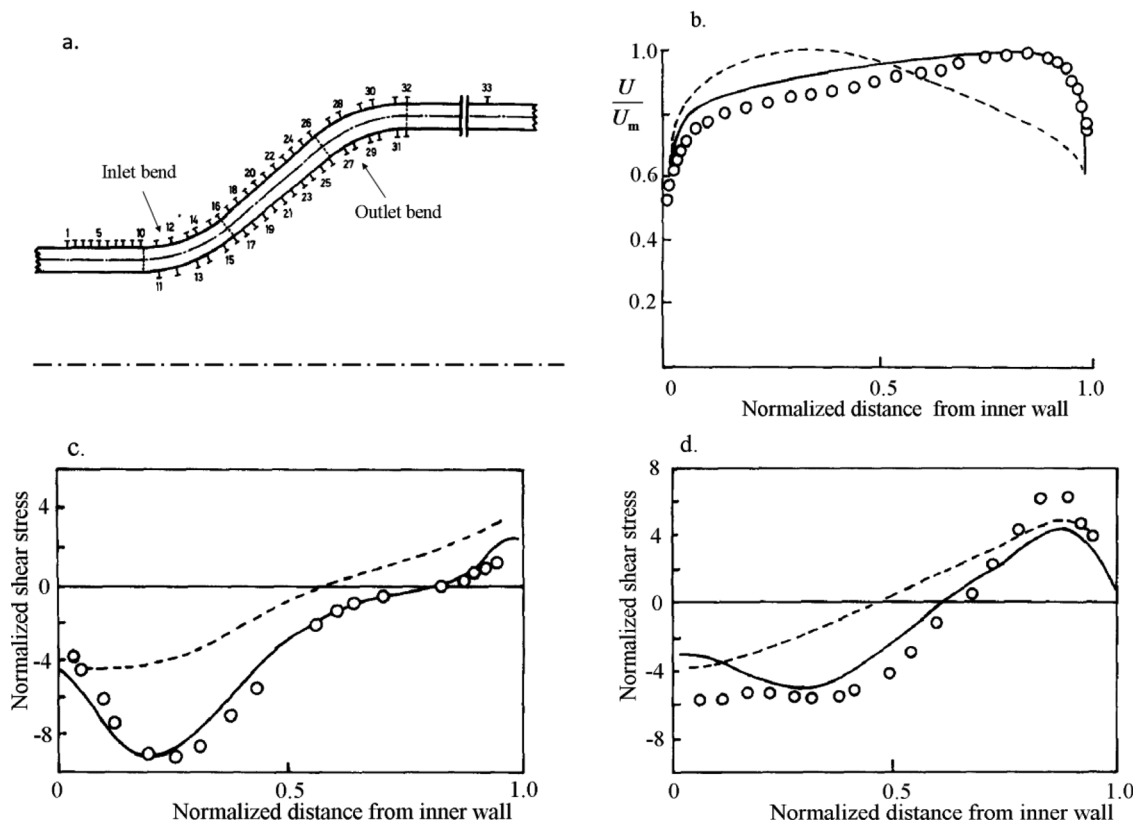
FIG. 2. Flow development through a faired diffuser: (a) annular flow configuration; (b) mean velocity at the exit from the diffuser; (c) and (d) shear stress profiles at the end of the inlet bend and at the end of a straight diffusing section, respectively. Symbols: experimental data, Stevens and Fry;[19] – – – computed using the k–ε linear eddy-viscosity model; ——— computed with the Basic Model (second-moment closure) Jones and Manners.[18] Reproduced with permission from K. Hanjalić and B. E. Launder, *Turbulence Modeling in Engineering and the Environment*. Copyright 2011 Cambridge University Press.

where here the symbol φ denotes the Reynolds stress $\overline{u_i u_j}$ with the coefficient c_φ usually assigned a value of approximately 0.2. In fact, comparison with the corresponding term in Eq. (3) shows that the kernel of Eq. (7) is not fully consistent with its role as a model of $-\overline{u_i u_j u_k}$

since, unlike the kernel, the latter is unaltered by re-sequencing the subscripts i, j, and k. While the potential impact of such infidelities should always be checked, they were not significant in the case reported. In Ref. 21, consistency was retained by adopting a more

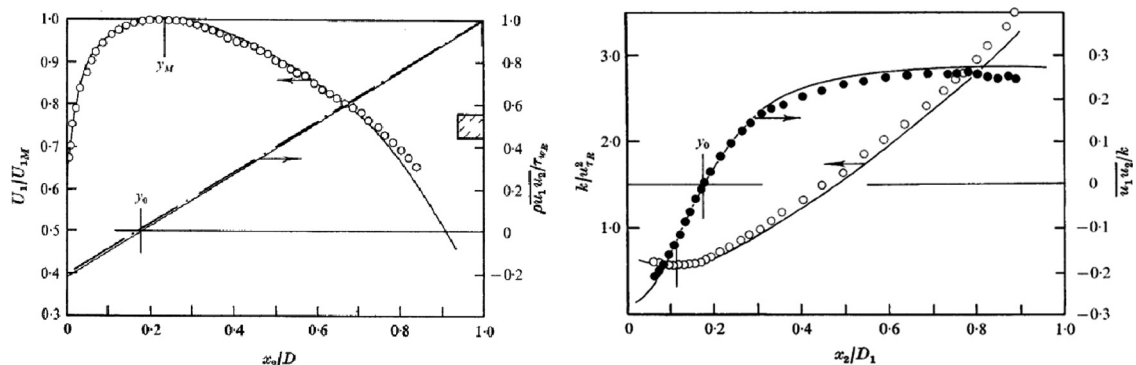FIG. 3. Fully developed flow through a plane channel with ribs on one wall. Symbols and chain line: experimental data, Hanjalić and Launder[20] Full lines: computations.[21] Note U_1, x_2, and $\overline{u_1 u_2}$ denote U, y, and $\overline{uv}$ in the present notation. Reproduced with permission from Hanjalić and Launder, J. Fluid Mech. **52**, 620 (1972) with the Copyright 1972, Cambridge University Press.

elaborate version comprising three such terms with the subscripts i, j, and k successively taking the role that k alone plays in the kernel of Eq. (7). The coefficient c_φ was thus correspondingly reduced.).

A weakness of Eq. (5) is that in a simple shear flow the normal stresses orthogonal to the direction of mean motion are equal. While not of great significance in many 2D free shear flows, in 3D flows, particularly near-wall flows, this very simple formulation is quite inadequate. Reference 21 had avoided that problem by generalizing Eq. (5) to what Naot *et al.*[23] subsequently called the "quasi-isotropic" linear model and even adding non-linear products. (The general linear formulation was independently discovered by several groups including the writers[21] and Lumley[25] though in practice it has been less successful than the IP model.) A more general approach to expanding the applicability of the pressure-strain approximation, however, was stimulated by a short note by Schumann[24] arguing that modeling proposals should be limited to forms that were *impossible* to lead to unachievable states of turbulence (sometimes termed "realizability constraints"), as, for example, negative normal stresses.

Lumley,[25] in a major contribution, took Schumann's proposal and from it developed a comprehensive modeling strategy that required compliance with what is often termed the "two-component limit," TCL. The idea is that *if* a normal stress should fall to zero in the course of a solution, the model should ensure that thereafter the rate of change would be greater than or equal to zero. As a complement to this approach, he introduced the second and third invariants of the anisotropic stress tensor), A_2 and A_3

$$a_{ij} \equiv \left(\overline{u_i u_j} - 2/3 \delta_{ij} k\right); \quad A_2 \equiv a_{ji} a_{ij}; \quad A_3 \equiv a_{ji} a_{ik} a_{kj}. \quad (8)$$

Most importantly, he showed that the composite invariant $A \equiv 1 - 9$ $[A_2 - A_3]/8$ (sometimes termed Lumley's flatness parameter) always vanished in two-component turbulence. With these weapons, he developed a nuanced elaboration of Φ_{ij1}[25] and a far more comprehensive representation of Φ_{ij2}, Shih and Lumley.[26] Broadly, the same route for modeling the latter was subsequently followed by Fu[27] though applying the TCL constraints somewhat differently. The formidable algebraic detail with both schemes is not appropriate for inclusion here but is given in the cited references and also in Craft and Launder.[28,29] A companion paper includes a parallel treatment for

stratified flows, of which more later. The model of Ref. 27 has been successfully applied to a wide range of challenging shear flows including the 3-dimensional wall jet by Craft and Launder,[29] Fig. 4, and the flow through a rectangular channel with partially roughened walls by Launder and Li.[30] In both cases, the resultant flow is dominated by the anisotropy of the Reynolds stresses acting in a plane orthogonal to the primary flow driving small but highly influential turbulence-driven secondary velocities in that plane. In the wall jet, these produced a spreading rate parallel to the wall some five times greater than that normal to it while, for the latter, illustrated in Fig. 5, major distortions of the axial velocity were created in close accord with measurements of Hinze.[31] By contrast, any isotropic eddy viscosity model would produce zero secondary motion in fully developed flow through a straight channel and a growth rate of the wall jet greater in the wall-normal direction than that parallel to the wall!.

An alternative approach to applying "realizability" constraints on the pressure-strain correlation that is algebraically less complex than the TCL schemes of Refs. 26 and 27 has been developed by Speziale *et al.*[32] It has been successfully applied to several homogeneous flows and wall-bounded, two-dimensional boundary layers achieving reasonable agreement with the normal stress profiles without including wall-proximity additions. Yet a further important route for making the turbulence model properly sensitive to the wall's proximity has been developed by Durbin.[33] That strategy is, however, most appropriately considered in the context of viscous and other near-wall effects on turbulence, the topic of Sec. IV.

III. THE TURBULENCE ENERGY DISSIPATION RATE, LENGTH, AND TIME SCALES

Readers will have noted that, in approximating the stress dissipation by viscous action and its diffusion, Eqs. (6) and (7), the turbulence energy dissipation rate was introduced, though that too was an unknown. A brief summary of routes adopted for its determination is now provided.

Originally ε had been approximated by direct analogy with the turbulence-energy transport equation, i.e., $Dk/Dt = \mathcal{D}_k + P_{kk}/2 - \varepsilon$. Thus,
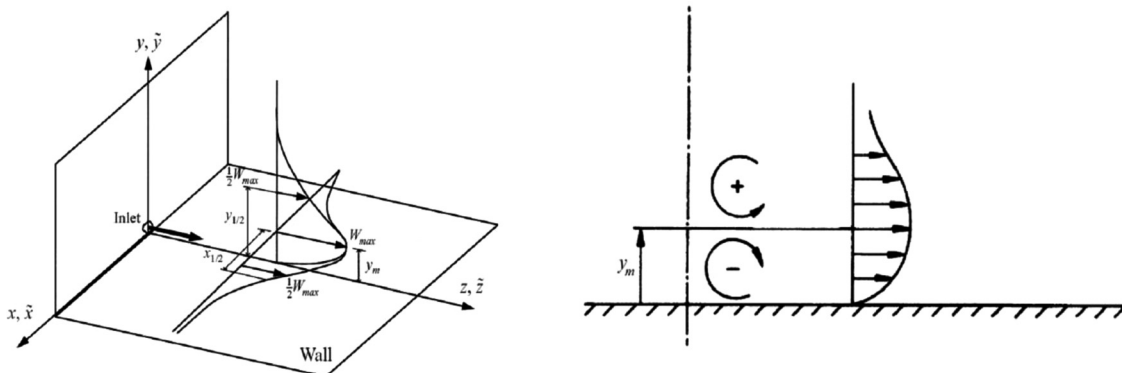

FIG. 4. Three-dimensional wall jet. Left: flow configuration, right: sketch of secondary flow in a cross-sectional plane generated by the anisotropy of the Reynolds stress in the plane orthogonal to the primary flow. Reproduced with permission from Craft and Launder J. Fluid Mech. **435**, 309 (2002). Copyright 2002 Cambridge University Press.
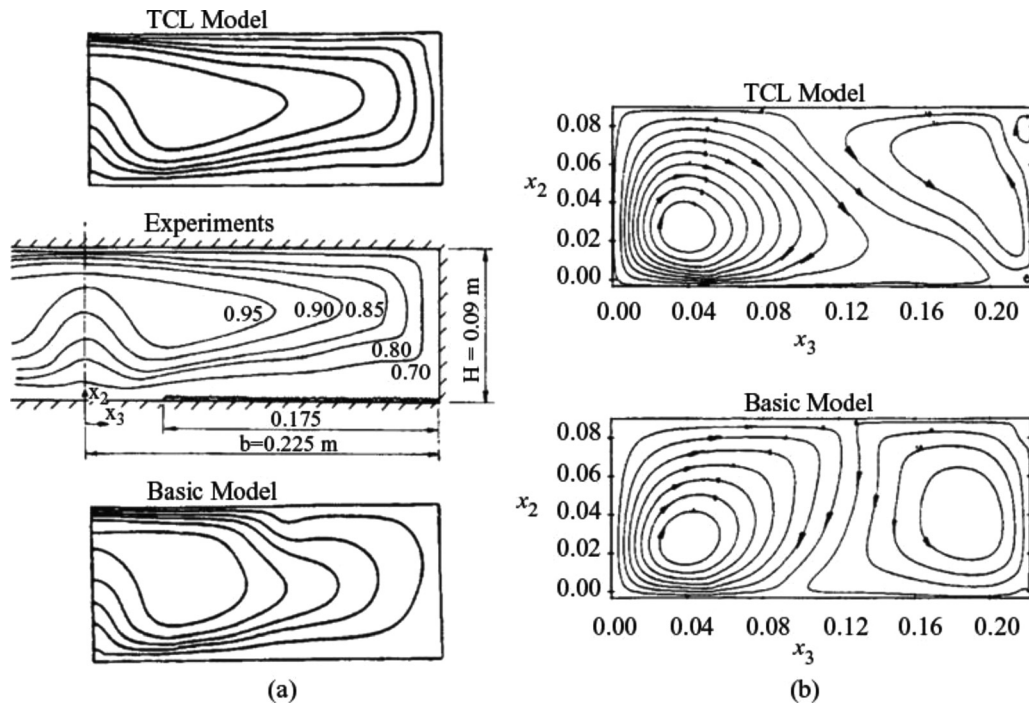
FIG. 5. Flow through a rectangular-sectioned duct with a partially roughened lower wall. (a) Contours of mean velocity: computations of Launder and Li,[30] experiments of Hinze;[31] (b) Predicted secondary flows. Reproduced from Launder and Li, Phys Fluids **6**, 1004 (1994) with the permission of AIP Publishing.

$$\frac{D\varepsilon}{Dt} = \mathcal{D}_\varepsilon + [c_{\varepsilon 1}\mathcal{P}_{kk}/2 - c_{\varepsilon 2}\varepsilon]\frac{\varepsilon}{k}, \tag{9}$$

where the empirical coefficients $c_{\varepsilon 1}$ and $c_{\varepsilon 1}$ were initially treated as constants (and still are in many codes) and the diffusion contribution was obtained by the GGDH approximation,

$$\mathcal{D}_\varepsilon = \frac{\partial}{\partial x_k}\left[c_\varepsilon \frac{\overline{u_k u_l}k}{\varepsilon}\frac{\partial\varepsilon}{\partial x_l}\right]. \tag{10}$$

The three unknown coefficients, $c_{\varepsilon 1}$, $c_{\varepsilon 2}$, and c_ε, were fixed by reference to experimental data (The present authors first proposed, a half century ago,[21] the three experimental flow test cases, still widely adopted, to fix the coefficients: grid turbulence decay; the spreading rate of the plane jet or mixing layer; and the 'universal' logarithmic region of the flat-plate boundary layer.). As the range of flows computed progressively widened, however, weaknesses began to emerge in the form of Eq. (9) and, naturally, numerous modifications to the original formulation were subsequently proposed. These have taken one of three general forms: (i) additional terms involving the mean velocity gradient have been added as a source;[34,35] (ii) the coefficient $c_{\varepsilon 2}$ was made a function of the stress invariants, Eq. (7);[25,36] near-wall constraints were added to prevent the near wall turbulent length scale (which may be taken as $k^{3/2}/\varepsilon$) departing too far from that found in a high-Reynolds-number, flat-plate boundary layer.[37,38] Perhaps the best that can be said of current versions of the ε equation is that because of its widespread use, its successes and weaknesses are widely known as are the adaptations (if any) to the standard version that are best suited for the class of turbulent flows that the user wishes to compute.

An alternative approach is to adopt a different variable from ε that might be more amenable to modeling. Again, there has been no shortage of such proposals, the best known and most promising choice being ω, a quantity proportional to (ε/k) proposed by Wilcox.[39] Unlike the basic dissipation equation, a gradient-diffusion approximation for the diffusion process does not cause the near-wall length scale to grow significantly as the flow approaches separation. It has been widely and successfully applied to thin shear flows and especially to boundary-layer flows developing toward and sometimes beyond separation.[40] It has thus been particularly widely applied to problems of flow over airfoils and other aerodynamic flows. Like the ε equation, however, it should not be seen as a panacea for determining the length and timescales of the energy-containing turbulent eddies. More extensive discussion and analysis on determining the alternative scaling quantities in turbulence may be found in Ref. 8.

IV. SECOND-MOMENT CLOSURE IN VISCOUS AND WALL-AFFECTED REGIONS (WIN MODELING)

Although not explicitly stated, all the test cases reported above have limited their coverage to regions where viscous or wall-proximity effects were unimportant. For flows past walls, that has meant that, in place of the no-slip boundary condition for all mean and turbulent velocity components that is strictly applicable at the wall itself, conditions have been applied just outside the region where viscous effects are important by using what are commonly termed "wall functions." Thus, for example, the mean velocity may be presumed to vary according to the well-known semi-logarithmic "law of the wall" with consistent assumptions regarding other dependent variables. While this

approach is attractively economical, it is by no means applicable to all flows of practical interest. This wall-adjacent region, while often referred to as "universal" (when scaled by the local wall shear stress and fluid properties), is anything but universal in practice!

The assumption of universality ceases to be accurate if the total shear stress (that is, viscous plus turbulent shear stress) changes significantly across the thin wall-adjacent layer where viscous effects are significant. Such situations arise at separation, in strongly accelerated flows or where force fields are important. It is to resolve such non-compliant flows that wall-integration (WIN) schemes have been developed. An early approach of this type by the present authors,[41] following the route of contemporary eddy-viscosity models, introduced a local turbulent Reynolds number $Re_t \equiv k^2/\nu\varepsilon$ (which vanishes at the wall) to reduce the Reynolds shear stress to zero at approximately the correct rate. (This scheme solved transport equations just for the shear stress and the turbulence energy while the individual normal stresses were obtained from algebraic connections with those quantities.) Several successful predictions were reported of laminarizing flows. Basing the turbulent Reynolds number on purely turbulent velocity ($k^{1/2}$) and length ($k^{3/2}/\varepsilon$) scales is important for alternative choices of Reynolds number (based on friction velocity and wall distance) within eddy-viscosity models had proved to be much less successful.

A more comprehensive treatment of the budget of the individual stress components was later provided in the work of Launder and Tselipidakis[42] and Hanjalić and Jakirlić.[43] Let us note that for an incompressible fluid, continuity requires that at a wall ($x_2 = 0$) $\partial u_2/\partial x_2 = 0$ since $\partial u_1/\partial x_1 = \partial u_3/\partial x_3 = 0$. That in turn implies that in the limit as $x_2 \to 0$,

$$\overline{u_1^2} \sim \overline{u_3^2} \sim x_2^2; \ \overline{u_2^2} \sim x_2^4; \ \overline{u_1 u_2} \sim x_2^3. \tag{11}$$

Indeed, these different exponents are well borne out by direct numerical simulations such as those of Hoyas and Jimenez[44] for fully developed flow in a plane channel.

Recognizing that close to a wall turbulence is populated largely by smaller-scale eddies, Hanjalić and Jakirlić[45] also included in their pressure-strain model the corresponding invariants E_2, E_3 and E of the stress-dissipation anisotropy where $E_2 \equiv e_{ij}e_{ij}$, etc., and $e_{ij} \equiv (\varepsilon_{ij}/\varepsilon -2/3\delta_{ij})$, with ε_{ij} evaluated from an algebraic function in terms of $\varepsilon, k, \overline{u_i u_j}$, and Re_t. This made it possible to reproduce the wall-limiting behavior of all stress components and thus, indirectly, the two-component limit. This scheme, hereafter denoted as the HJ model, was subsequently successfully applied to a number of attached and separating wall-bounded flows including cases of laminar-to-turbulent and reverse transition, rotating and swirling flows, e.g., Hanjalić et al.,[46,47] Jakirlić and Hanjalić.[48] Figure 6 shows, for example, the variations of skin friction in an oscillating boundary layer over a range of Reynolds numbers based on the Stokes thickness, δ_S. It is noted that the final development of this work sprang from a paper by Jovanović et al.[49] that began with the transport equation for the two-point velocity correlation and ended with the proposal to replace the stress dissipation rate ε_{ij} by what they termed the *homogeneous dissipation rate*, $\varepsilon_{ij}^h = \varepsilon_{ij} - (1/2)\nu\partial^2\overline{u_i u_j}/\partial x_j^2$. Jakirlić and Hanjalić[50] developed this idea using the corresponding "homogeneous" dissipation rate of turbulence energy $\varepsilon^h = \varepsilon - (1/2)\nu\partial^2 k/\partial x_j^2$ and showed that this allowed the exact wall limits of ε_{ij} to be satisfied for all components without using any wall-configuration parameters such as wall-normal unit vectors used in earlier models.

A different and powerful approach to accounting for non-local, inviscid wall effects has been taken by Durbin.[51] As noted in Sec. II, he had realized that the major effect of a solid wall on the pressure fluctuations in the wall's vicinity arose principally from non-local, inviscid blocking, rather than simply viscous effects. Thus, as an extension of his elliptic-relaxation strategy, Durbin[51] determined the pressure-strain term, Φ_{ij}, from

$$\Phi_{ij} - L^2\nabla^2\Phi_{ij} = \Phi_{ij}^h \tag{12}$$

where the "homogeneous" part, Φ_{ij}^h, can in principle be chosen as any pressure-strain model unaffected by wall proximity [e.g., Eqs. (4) and (5)]. Equation (12) has an elliptic character implying that the Laplacian ∇^2 will account for the conditions on the solid or free surface bounding the flow domain. The characteristic turbulent length scale, L, may, sufficiently far from a wall or free surface, conveniently be taken as $k^{3/2}/\varepsilon$. With the appropriate boundary conditions, Eq. (12) preserves the non-local character of the pressure-strain term and exerts damping due to wall blocking via elliptic differential equations rather than as an algebraic expression in terms of local quantities and wall distance or by the use of stress invariants. Equation (12) was then recast in terms of an elliptic relaxation (ER) function f_{ij} defined as a ratio of a group of terms in the stress transport equation, which in addition to Φ_{ij}^h also included pressure diffusion and ε_{ij}.

While Durbin's ER strategy of adapting Φ_{ij}^h to include near-wall effects attracted immediate attention, some shortcomings were identified and several alternative versions proposed, Wizman et al.,[52] Manceau and Hanjalić,[53] and Manceau et al.[54] Yet, none of these removed the major drawback: the large number of auxiliary equations for f_{ij}. This challenge led Manceau and Hanjalić[55] to devise an *elliptic blending model* (EBM) with a *scalar* elliptic relaxation function α. The pressure-strain term was taken as a blending of the near-wall and far-from-the-wall forms of Φ_{ij},

$$\Phi_{ij} = (1 - \alpha^2)\Phi_{ij}^w + \alpha^2\Phi_{ij}^h \tag{13}$$

The ellipticity of the model is achieved by solving an elliptic differential equation for the blending function: $L^2\nabla^2\alpha - \alpha = -1$, satisfying the conditions $\alpha = 0$ at the wall and unity very far away from it. In Eq. (13), Φ_{ij}^h can be any homogeneous model, whereas an expression was proposed for Φ_{ij}^w in terms of wall-normal unit vectors. Figure 7 shows results from Manceau[56] of computations of the EBM applied to fully developed channel flow for three levels of orthogonal-mode rotation (plus the non-rotating case) compared with the LES results of Lamballais et al.[57]

The shift of the position of maximum velocity initially toward the suction surface as the rotation rate is progressively increased is very well captured while, at the highest spin rate at which measured data are available, there is a shift back toward the pressure surface. In terms of the wall shear stresses, the suction-surface friction velocity is rapidly reduced by rotation while, initially, that on the pressure surface is raised. Further increase in the rotation, however, produces a steep decline in U_τ on the pressure surface too, leading eventually to a laminarized flow in which the wall stress is essentially the same on both surfaces. All these features are accurately captured by the closure model. Of course, had one used an isotropic eddy-viscosity model, for
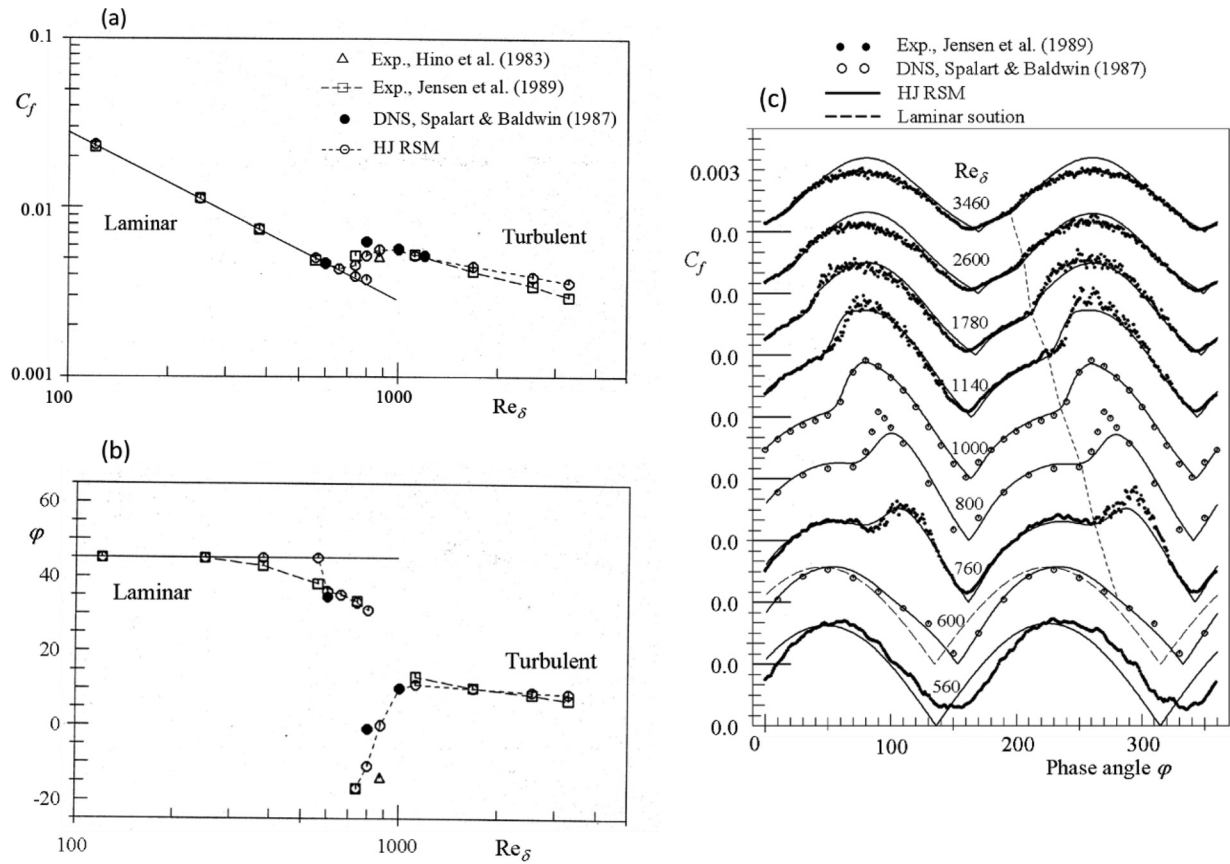
FIG. 6. Oscillating boundary layer over a range of Re_{δ_s} (based on the Stokes thickness $\delta_s \equiv \sqrt{2\nu/\omega}$ and maximum free stream velocity): (a) friction factor, (b) phase lead of the maximum wall shear stress vs maximum free-stream velocity, and (c) variation of wall shear stress through a cycle, Hanjalić *et al.*[46] Reproduced with permission from K. Hanjalić and B. E. Launder, *Turbulence Modeling in Engineering and the Environment*. Copyright 2011, Cambridge University Press.[8]

all rotation rates the wall stresses and velocity profiles would have been precisely the same as for the non-rotating case since there is no Coriolis term in the k or ε equations!

V. STRATIFIED FLOWS

The foregoing example provides a dramatic illustration of how the action of a force field (in that case a Coriolis force) in the stress-transport equation can hugely alter a flow's character. An even greater diversity of effects may arise from the actions of the gravitational field. In that case, the kinematic fluctuating force in the instantaneous velocity equation, given by $f_i \equiv \rho' g_i / \rho$, is conveniently expressed in terms of temperature fluctuations so that the force-field term in Eq. (3) for the turbulent stress transport becomes

$$\mathcal{F}_{ij} \equiv \mathcal{G}_{ij} \equiv \left(\overline{\rho' u_j} g_i + \overline{\rho' u_j} g_j \right) \Big/ \rho = -\beta \left(\overline{\theta u_j} g_i + \overline{\theta u_i} g_j \right), \quad (14)$$

where β denotes the expansion coefficient defined by $\beta \equiv -(1/\rho) (\partial \rho / \partial \Theta)|_P$ and the P subscript indicates that the derivative with respect to temperature is at constant pressure.

To close the mean temperature equation,

$$\frac{\partial(\rho\Theta)}{\partial t} + \frac{\partial(\rho U_j \Theta)}{\partial x_j} = S_\Theta + \frac{\partial}{\partial x_j}\left(\gamma \frac{\partial \Theta}{\partial x_j} - \overline{\theta u_j} \right), \quad (15)$$

but also to determine the gravitational source $\mathcal{F}_{ij}$ in Eq. (3) via Eq. (14) at the same second-moment-closure level, a transport equation for the turbulent heat (and/or other scalar) flux is needed, which can be derived following the analogous steps as in developing Eq. (3):

$$\frac{D\overline{\theta u_i}}{Dt} \equiv \underbrace{\frac{\partial \overline{\theta u_i}}{\partial t}}_{\mathcal{L}_{\theta i}} + \underbrace{U_k \frac{\partial \overline{\theta u_i}}{\partial x_k}}_{\mathcal{C}_{\theta i}}$$

$$= -\underbrace{\left(\overline{u_i u_j}\frac{\partial \Theta}{\partial x_j} + \overline{\theta u_j}\frac{\partial U_i}{\partial x_j} \right)}_{\mathcal{P}_{\theta i} = \mathcal{P}_{\theta i}^\Theta + \mathcal{P}_{\theta i}^U} + \underbrace{\frac{1}{\rho}\sum_n \overline{\theta f_i^n}}_{\mathcal{F}_{\theta i}} + \underbrace{\frac{1}{\rho}\overline{p\frac{\partial\theta}{\partial x_i}}}_{\Phi_{\theta i}}$$

$$- \underbrace{(\alpha+\nu)\overline{\frac{\partial\theta}{\partial x_k}\frac{\partial u_i}{\partial x_k}}}_{\varepsilon_{\theta i}} + \underbrace{\frac{\partial}{\partial x_k}\left[\overline{\alpha u_i \frac{\partial\theta}{\partial x_k}} + \overline{\nu\theta\frac{\partial u_i}{\partial x_k}} - \overline{\theta u_i u_k} - \frac{1}{\rho}\overline{p\theta}\delta_{ik} \right]}_{\mathcal{D}_{\theta i}^\alpha + \mathcal{D}_{\theta i}^\nu + \mathcal{D}_{\theta i}^t + \mathcal{D}_{\theta i}^p}.$$
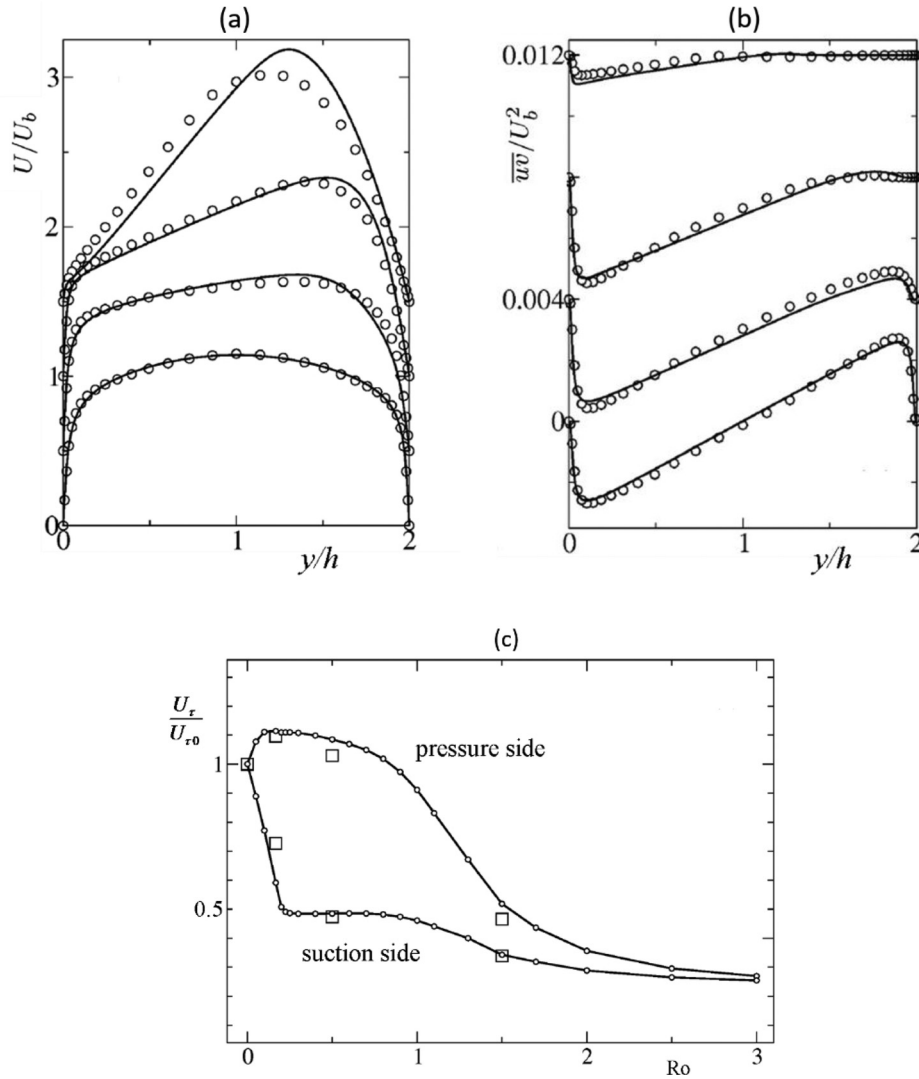
$$(16)$$

FIG. 7. Computations of flow in a plane channel at Re = 7000 rotating around a spanwise axis for a range of rotation numbers (Ro = 0, 0.16, 0.5, and 1.5). (a) mean velocity, (b) turbulent shear stress, and (c) wall friction velocities. Symbols: LES Lamballais et al.;[57] lines: EBM model. Reproduced with permission from Manceau, *Proceedings 4th International Symposium on Turbulence & Shear Flow Phenomena*, 259–264 (2005). Copyright 2005 R. Manceau.

As with Φ_{ij} in the stress-transport equation, the pressure/scalar-gradient correlation, $\Phi_{\theta i}$, is a crucial term to model. Again the process needs to contain purely turbulence, mean-strain and force-field contributions. There is a wide range in the algebraic complexity of alternative models ranging from the very simple counterparts of Eqs. (4) and (5),

$$\Phi_{\theta i 1} = -c_{1\theta}\frac{\varepsilon}{k}\overline{\theta u_i}; \quad \Phi_{\theta i 2} = c_{2\theta}\overline{\theta u_k}\frac{\partial U_i}{\partial x_k} = -c_{2\theta}\mathcal{P}^U_{\theta i}, \quad (17)$$

to the far more complex two-component-limit forms that satisfy various extreme states of the scalar flux field.[8,28] (Notice that in the simple model of $\Phi_{\theta i 2}$ shown in Eq. (17), only the part of the scalar-flux production containing mean velocity gradients is included. While that is the usual practice, variations exist (e.g., Ref. 58), reflecting the fact that such simple approximations are inevitably of limited validity.) As one would hope, there is a demonstrated broadening of the range of flows

covered as the model complexity is raised. Here, however, we forego any examination of the models' performance where the scalar's role is passive in favor of considering more complex stratification effects.

A complete second-moment closure of the momentum and energy Eqs. (1) and (15) for flows involving significant thermal and/or concentration stratification entails solving Eqs. (3) and (16) together with the scale-determining variable for which, in most applications, the energy dissipation rate, ε, Eqs. (9) and (10), has been adopted. Moreover, since the gravitational source in the scalar-flux equation, (16), becomes $\mathcal{F}_{i\theta} \equiv \mathcal{G}_{i\theta} \equiv \overline{f_i\theta} = -\beta g_i\overline{\theta^2}$, a transport equation for the mean square temperature variance, $\overline{\theta^2}$, is also required. That is readily obtained (Corrsin[59]) by multiplying the unsteady equation for the transport of a scalar, $\hat{\Theta}$, by twice the fluctuating scalar, 2θ, and averaging

$$\frac{D\overline{\theta^2}}{Dt} \equiv \underbrace{\frac{\partial \overline{\theta^2}}{\partial t}}_{\mathcal{L}_{\theta\theta}} + \underbrace{U_j \frac{\partial \overline{\theta^2}}{\partial x_j}}_{\mathcal{C}_{\theta\theta}} = \underbrace{-2\overline{\theta u_j}\frac{\partial \Theta}{\partial x_j}}_{\mathcal{P}_{\theta\theta}} - \underbrace{2\alpha\overline{\left(\frac{\partial \theta}{\partial x_j}\right)^2}}_{\varepsilon_{\theta\theta}} + \underbrace{\frac{\partial}{\partial x_j}\left(\alpha\frac{\partial \overline{\theta^2}}{\partial x_j} - \overline{\theta^2 u_j}\right)}_{\mathcal{D}_{\theta\theta}}.$$

$$(18)$$

(Here, α denotes the fluid's thermal diffusivity.) The equation closely resembles that for the turbulence energy save for the absence of pressure diffusion, with the terms having an analogous physical meaning to those in Eq. (3).

Now, compared with a linear eddy viscosity model, Eq. (2) and its equivalent for the scalar flux,

$$\overline{\theta u_i} = -\alpha_t \frac{\partial \Theta}{\partial x_i}, \qquad (19)$$

a full second-moment closure may look overly complicated and computationally too demanding. However, the inter-connectivity of the various stress and heat-flux components gives a strong indication of the physical complexities that may arise between the two fields. The couplings among the different contributors to the equation set and the way their interaction changes depending upon the orientation of the flow is illustrated schematically in Fig. 8. It compares the inter-couplings arising in a two-dimensional thin shear flow orientated horizontally and vertically. For both situations, x_1 is the mean flow direction and x_2 the direction in which the mean velocity and density vary. The lines indicate coupling between the respective second moments, the arrows indicating that the second moment at the upstream end of any line contributes to generating the component at the downstream end.

In modeling the crucial pressure-strain term in stratified flows, some groups[60,61] initially neglected any influence of gravitational forces on the process (which was logical since the other linear process, the mean-strain influence, was also neglected). Following the appearance of the IP model, however, Ref. 14 and many later contributions applied the same approximation strategy to account for the "redistribution" of gravitational stress generation,

$$\Phi_{ij3} = -c_3\left(\mathcal{G}_{ij} - \mathcal{G}_{kk}\delta_{ij}/3\right) \qquad (20)$$

where now there is no strict need (as there was with a Coriolis force) to make the proportionality coefficient the same as for Φ_{ij2}. Nevertheless, the value of c_3 has in practice usually been taken equal to or close to that of c_2 with values in the range of 0.5–0.6. The analogous IP arguments applied to the pressure-temperature gradient product in the heat-flux equation, Eq. (16), lead to

$$\Phi_{\theta i3} = -c_{3\theta}\mathcal{G}_{\theta i} = +c_{3\theta}\beta g_i \overline{\theta^2}. \qquad (21)$$

The coefficient $c_{3\theta}$ is normally assigned the same value as $c_{2\theta}$ of about 0.5, e.g., Ref. 14.

As an early application of the approach, Fig. 9, compares predictions with the IP model for the case of a nominally homogeneous, stably stratified, free shear flows measured by Webster.[62] The strength of the stratification is expressed in terms of the flux Richardson number R_f, defined as the ratio of the rate of removal of turbulence energy by working against gravity to that supplied by mean-strain action. (The *gradient* Richardson number, Ri, is R_f multiplied by the Prandtl number). The left figure shows that, as the stable stratification gets stronger, the proportion of fluctuating energy in the vertical direction decreases while that in the stream direction increases, a feature that is well captured by the model. So far as the heat fluxes are concerned, Fig. 9(b) indicates that vertical heat transport is very severely reduced relative to the streamwise heat flux with increasing stable stratification.

Just as with Φ_{ij2} and $\Phi_{\theta j2}$, TCL constraints have also been applied to the buoyant parts of the non-dispersive pressure correlations Φ_{ij3} and $\Phi_{\theta j3}$ in order to obtain a still more widely applicable model. The analyses presented in Craft *et al.*[63] and Craft and Launder[64] include examples of application to several buoyantly modified shear flows that showed a generally superior performance of the TCL approach compared with the basic IP model, especially in more challenging strongly inhomogeneous cases. An illustrative example is the negatively buoyant wall jet shown in Fig. 10(a): a downward directed plane wall jet of warm water is injected parallel to the wall into a slowly upward moving cool stream, causing the wall jet to break away from the wall, reversing its direction. Figure 10(b) compares RANS predictions using the TCL and the IP-based (Basic) approaches with the LES results by Addad *et al.*[65] [In both cases, the more successful treatment of the wall sublayer (the "AWF scheme") is used.] While neither scheme captures fully the level of mixing exhibited by the LES, the TCL model clearly achieves the better performance and far better than results with a linear eddy viscosity model (not shown).

As the foregoing has suggested, the early development of second-moment closure applied to stratified flows revolved around issues of how to account for gravitational effects in the resultant model, usually by reference to relatively simple laboratory-based flows. At about the same time, however, there appeared several publications from research groups in the USA, specifically focused on atmospheric flows, e.g., the already noted Refs. 60 and 61 as well as, *inter alia*, Donaldson,[66] Mellor and Yamada,[67] Wyngaard,[68] and Lewellen *et al.*[69] Although recognizing that higher-order-closure models provided a better basis
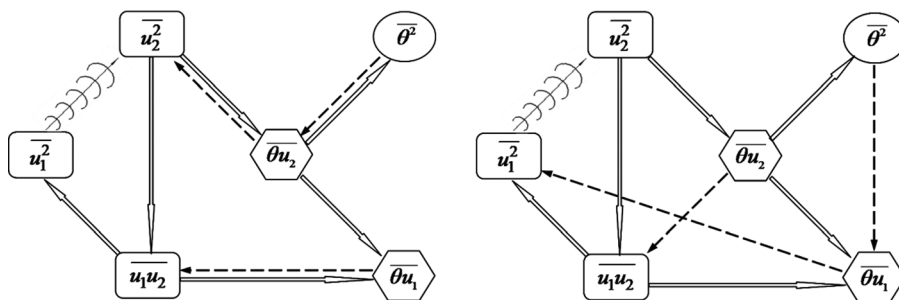

FIG. 8. Contrasting buoyant couplings among the second moments in horizontal (left) and vertical (right) two-dimensional thin shear flows. Broken arrows indicate buoyant coupling; full arrows denote coupling through mean velocity/scalar gradient; pressure-strain coupling is indicated symbolically by "waves." Reproduced with permission from K. Hanjalić and B. E. Launder, *Turbulence Modeling in Engineering and the Environment.* Copyright 2011 Cambridge University Press.[8]
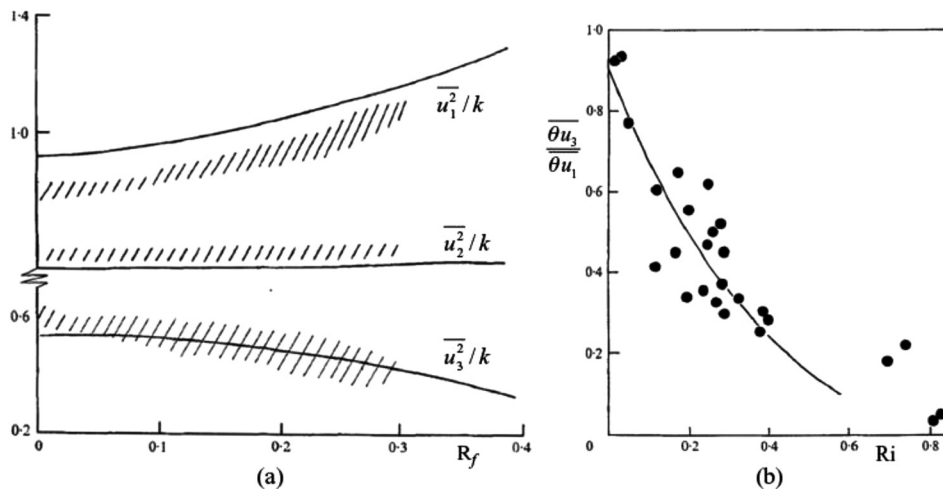
FIG. 9. Normal stresses and heat fluxes in stable stratification. (a) Relative normal stress levels as a function of flux Richardson number. (b) Variation of vertical to streamwise heat flux with gradient Richardson number. Symbols/shading, experiments (Webster[62]) lines, computations. Note: x_1 denotes the main flow direction (horizontal); x_3 vertical. Reproduced with permission from Webster, J. Fluid Mech. **67**, 574 and 579 (1975). Copyright 1975 Cambridge University Press.

for representing the physics of turbulence than was possible with eddy-diffusivity approximations, most early workers acknowledged that with the state of the art and the computing facilities of the time such a comprehensive approach was not practicable for real atmospheric meso- or regional scales requiring three-dimensional models that "can quickly get out of hand computationally."[68] Thus, a complete second-moment closure model in differential form was considered primarily as the basis for developing and parameterizing simpler versions (The spirit of the time, especially in the atmospheric community, was reflected in Wyngaard:[68] "Unfortunately, however, there is little theoretical guidance for the rational, systematic formulation of closure approximations. As discussed by Bradshaw, one can check the effects of closure assumptions by comparing calculations with detailed

measurements, but rarely are there data suitable for testing the closure assumptions themselves. Not surprisingly, then, models change as new flows are calculated and compared with data."). Yet, to demonstrate its benefits, Wyngard[68] applied a "full" model that included the correlations involving pressure fluctuations, though (as with other US contemporary contributors cited above) only the "slow parts," Φ_{ij1} and $\Phi_{\theta i1}$, Eqs. (4) and (17) were included in the model. He computed several simple cases of the horizontally homogeneous flows permitting sweeping approximations, with the two-dimensional mean velocity governed solely by geostrophic wind. The structure of the evolving nocturnal planetary boundary layer (PBL) was explored with the model by starting from initial conditions typical of a decaying convective PBL at the instant of transition. The author concluded that the
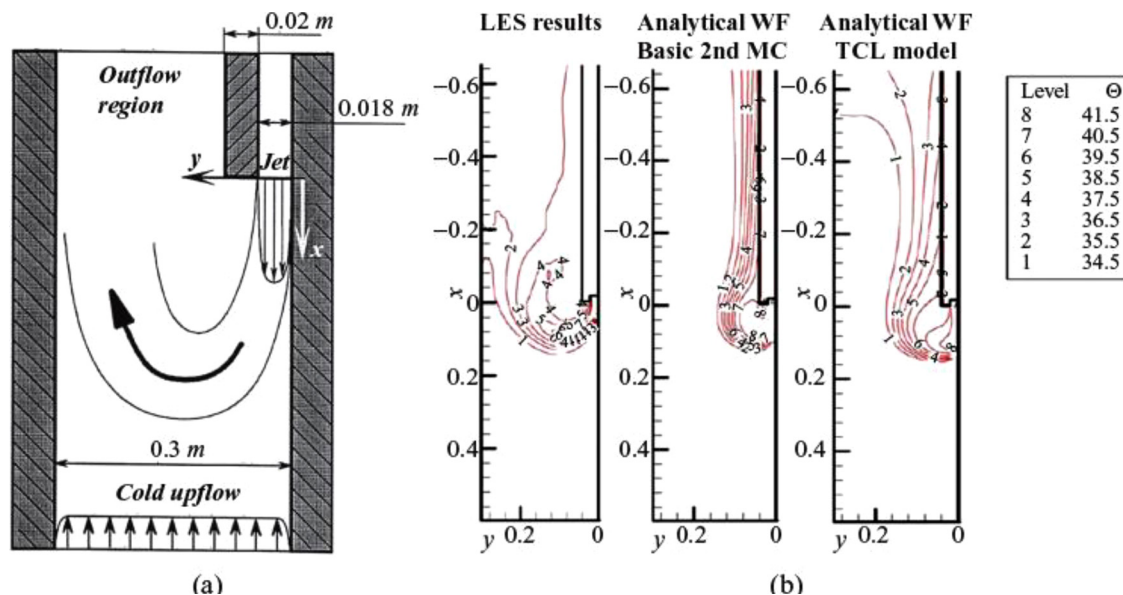

FIG. 10. Temperature contours for the negatively buoyant wall jet, comparison of different models: (a) flow configuration and (b) RANS computations, Craft et al.,[63] LES data from Addad et al.[65] Reproduced with permission from K. Hanjalić and B. E. Launder, *Turbulence Modeling in Engineering and the Environment*. Copyright 2011 Cambridge University Press.[8]

calculated surface-layer profiles of wind shear and temperature gradient agreed well with field data (the 1968 Kansas measurements).

Lewellen, *et al.*[69] reported the application of a full second-moment model (accounting, just as Wyngaard,[68] only for the "slow" terms, Φ_{ij1} and $\Phi_{\theta i1}$) to several simple (two-dimensional unsteady and three-dimensional steady) stratified flows including an atmospheric boundary layer subjected to diurnal variation from stable to unstable conditions.

A little earlier, Mellor and Yamada[67] published a general second-moment closure scheme for temperature-stratified flows, but focused on a systematic simplification of the general model aimed at discerning "a level of complexity which is intuitively attractive and which optimizes the computational speed and convenience without unduly sacrificing accuracy." The hierarchy of models was graded according to the degree of anisotropy (presumably, of the turbulent stress field) in four levels. The most complex, full second-moment closure (level 4) consists of 10 differential transport equations for the turbulence second moments ($\overline{u_i u_j}$, $\overline{\theta u_i}$, and $\overline{\theta^2}$) in addition to the mean momentum and energy equations (though, as noted below, not for the turbulent length scale or equivalent). Two versions of algebraic truncation (levels 2 and 3) were arrived at by dispensing with the differential convection and (partly) the diffusion terms in the stress and heat flux equations, while the simplest, eddy-viscosity/diffusivity model, Level 1, dispensed with all 10 differential equations. The authors focused on a planetary boundary layer subjected to a sinusoidal diurnal variation of the surface heat flux or temperature. Perplexingly, the authors reported that *all models gave nearly the same results*—an outcome that contradicts the subsequent findings by other authors, admittedly in different configurations of engineering relevance (e.g., Dol *et al.*,[71] Hanjalić,[72] to which we return below).

The treatment of the characteristic turbulence scale in these early models is also controversial. While Wyngaard used the standard ε equation, Mellor and Yamada[67] introduced several length scales appearing in different terms of the modeled equations, which were all assumed to be proportional to each other. The representative ("master") scale was prescribed algebraically assuming a linear variation from the ground, thus avoiding the need to solve a transport equation for a scale-providing variable. Lewellen *et al.*[69] followed Rotta's approach and proposed a transport equation for a length scale based on the integral of the two-point velocity correlation. Some years later, Mellor and co-workers[70] opted for the kL equation of Rotta, arguing that the ε equation is "fundamentally wrong since a small-scale parameter like ε cannot describe a macro-scale of turbulence" (Umlauf and Burchard[73]). This argument was repudiated by many other workers (e.g., Rodi[74]) on the grounds that the dissipation rate was primarily determined by the successive break-down of larger scale eddies to successively finer scales—a process clearly caused or, at least, modified by macro-scale actions.

VI. REDUCED, FASTER VERSIONS

A perennial question raised by users of CFD codes has been: Is there any way one can better capture the sensitivity of turbulent stresses to a complex strain or to force fields without having to use stress-transport models? Certainly, in the early 1970s, abandoning the concept of eddy viscosity and solving modeled versions of the stress-transport equations was (as noted above in the context of the atmospheric boundary layer) seen by the general CFD community as a step

too far, as much as for conceptual reasons as for the additional computational cost. However, Rodi[75] proposed that a significant simplification of the stress transport equations could be achieved by linking the transport terms to the transport of turbulence energy via the approximation

$$\frac{D\overline{u_i u_j}}{Dt} - \mathcal{D}_{ij} \approx \frac{\overline{u_i u_j}}{k}\left(\frac{Dk}{Dt} - \mathcal{D}_k\right) = \frac{\overline{u_i u_j}}{k}(\mathcal{P}_{kk}/2 - \varepsilon), \quad (22)$$

Where $\mathcal{D}_\varphi$ denotes the net diffusion rate of φ. With this assumption (sometimes referred to as "the weak non-equilibrium hypothesis"), the set of hitherto differential equations was reduced to algebraic form. So, if one adopts Eqs. (4) and (5a) for the pressure-strain model (as Rodi did) the resultant stress-strain connection is obtained as

$$a_{ij} = \alpha(\mathcal{P}_{ij} - \mathcal{P}_{kk}\delta_{ij}/3)/\varepsilon, \quad (23)$$

where the value of the constant coefficient α is linked to the choice of coefficients in Eqs. (4) and (5a). This type of model is generally referred to as an *algebraic stress model* (ASM). The resultant algebraic set for the stresses was, however, implicit rather than explicit. This did not matter in a marching solution of the thin-shear-flow equations (because the stresses appearing in $\mathcal{P}_{ij}$ were then taken as their already-determined values at the upstream node). Rodi and Scheuerer[76] showed that approximation produced results for curved shear layers very close to the earlier computations employing a full second-moment closure (with the same model for dissipation and pressure strain), both of which captured the reduction in spreading rate in the curved region displayed by experiments but missed by the linear eddy-viscosity computations. A similar reduction of the stress-transport equations to algebraic form had earlier been made by Launder and Ying[77] to obtain the first prediction of turbulence-driven secondary flows in square ducts. In that case, however, the transport terms made only a tiny contribution to the stress budget.

Nevertheless, it is noted that, especially in axisymmetric free shear flows where transport effects are usually more important than in wall-dominated flows, such algebraic stress models cannot be relied on to mimic the results of a complete second-moment closure. A particularly sensitive case is the round jet in a stagnant stream examined by Fu *et al.*;[78] for, while the numerical computation is simple, the turbulence field in this flow is strained in complex ways. Here, the ASM scheme returned peak shear stress levels 40% higher than the second-moment closure it attempted to imitate!

If one turns to fully elliptic flows, the quasi-explicit strategy for solving the ASM equations without iteration is no longer available. Moreover, the appearance of stress components as what amounted to source terms meant that the equations were commonly unmanageably stiff, requiring more iterations to convergence than the full transport equations. As a step toward removing this problem Pope[79] began the task of converting the implicit ASM set into an explicit set of equations, though the algebraic complexity meant that attention was confined to two-dimensional flows. Subsequently Gatski and Speziale,[80] with the help of *Mathematica*™ (Wolfram[81]) developed a general transformation for any linear pressure-strain model (see also Gatski and Rumsey[82] for a detailed presentation). The outcome of their work was an explicit formula for the stresses as a function of the strain (the usual linear term) and quadratic product groups of mean-strain and mean-vorticity tensors. A later formulation of the same type due to

Wallin and Johansson[83] has also become popular. While the approaches followed in these papers were termed "explicit algebraic stress models" (EASM) and had a clear analytical development with directly traceable physical assumptions, their final form was not different from the numerous semi-empirical models of the same type that are usually termed "non-linear eddy-viscosity models" (NLEVMs), reviewed in Ref. 8.

As already noted in Sec. V, analogous simplifications in the treatment of the second-moment transport terms have also been made by those concerned with flows strongly dependent upon the gravitational field, e.g., Mellor and Yamada.[67,70] Their so-called level 3 and level 2 1/2 are essentially the algebraic stress/flux models obtained by omitting the convection and diffusion terms from the differential transport equations, with somewhat different models of the pressure-containing covariances, but closed with empirically defined length scales. A distinction between levels 3 and 2 1/2 is in the treatment of the scalar variance $\overline{\theta^2}$: while at level 3 the modeled differential transport equation for $\overline{\theta^2}$, Eq. (18), is solved, level 2 1/2 employs a simple gradient model, $\overline{\theta^2} \propto \overline{\theta u_i} \partial \Theta / \partial x_i$. The latter expression obviously fails in a well-mixed layer above a heated surface where the mean temperature is essentially uniform. This fundamental weakness can be overcome by treating the problem as inherently unsteady, i.e., by solving the ensemble-averaged variables in time when the resolved stress and heat flux generated by large-scale convective structures recover a realistic field of $\overline{\theta^2}$ and other second-moments (Hanjalić[72]) as discussed in Sec. VII.

Algebraic models based on truncation of the differential second-moment transport equation but retaining all production and modeled pressure-covariance terms have also proved very useful in modeling flows driven or affected by buoyancy, especially in the fluid layer over a horizontal, unstably heated surface (known as the *penetrative convective mixed layer*), as also found in the classic Rayleigh–Bénard convection (with the fluid trapped between the heated bottom and cooled top

horizontal walls), e.g., Hanjalić.[72] Obviously, as noted above, the vertical heat or mass fluxes cannot be modeled in terms of the mean temperature or concentration gradient as assumed by eddy-diffusivity models. However, Fig. 11 shows that even a truncated algebraic flux model (AFM) obtained by neglecting the transport terms in the scalar-flux transport equation, Kenjereš[89] and Kenjereš and Hanjalić,[84] i.e.,

$$\overline{\theta u_i} = -\frac{1}{c_{1\theta}}\frac{k}{\varepsilon}\left[\overline{u_i u_j}\frac{\partial \Theta}{\partial x_j} + c'_{2\theta}\overline{\theta u_j}\frac{\partial U_i}{\partial x_j} + c'_{3\theta}\beta g_i\overline{\theta^2}\right], \quad (24)$$

(with the empirical coefficients $c_{1\theta}, c'_{2\theta}, c'_{3\theta}$ taken from the model of the full transport equation for $\overline{\theta u_i}$) meets the challenge well. We note that here the mean velocity is zero and the mean temperature essentially uniform; thus, the only non-zero source in the equation for the turbulent heat flux is the third term representing buoyant production. The scalar variance, $\overline{\theta^2}$, is obtained from the solution of its own transport equation. Clearly, no eddy-diffusivity model can adequately model the scalar flux since such schemes link heat fluxes purely to temperature gradients; that is why the "GGDH" predictions in Fig. 11(a) exhibit spurious temperature gradients in the mixed layer. For completeness, the vertical heat flux presented in Fig. 11(b) shows the close accord between the algebraic and differential second-moment closures (the latter denoted "DSM-DFM") though, interestingly, in the flux-reversal zone at the top of the mixed layer the algebraic version aligns more closely with the LES data of Schmidt and Schumann[85] while the differential version follows more closely the early experimental data of Deardorff et al.[86] (A full second-moment study of mixed layers achieving satisfactory agreement with data was also reported by Zeman and Lumley[87])

For more complex three-dimensional stratified flows where both the velocity and temperature fields are non-uniform, capturing the turbulent stress components may be essential to reproduce accurately the heat flux. A reduced algebraic stress model consistent with that for the
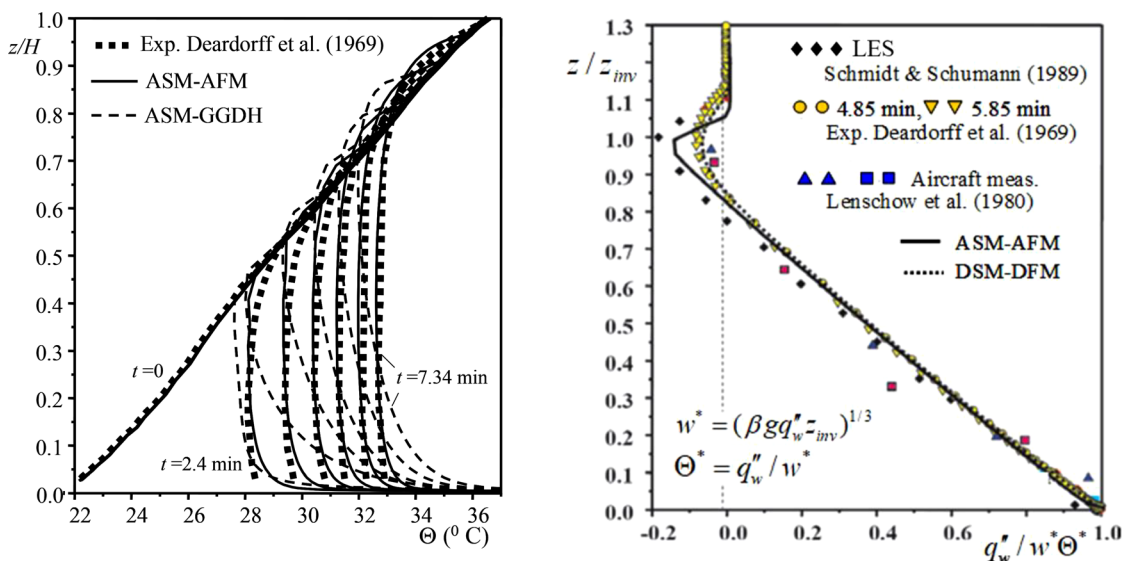

FIG. 11. Penetrative convection into an initially thermally stable layer heated from below. Left: the mean temperature field at $t = 0$, 2.40, 3.38, 4.38, 5.36, 6.39, and 7.34 min after the onset of bottom heating. Right: vertical heat flux. From Kenjereš & Hanjalić.[84] Reproduced with permission from K. Hanjalić and B. E. Launder, *Turbulence Modeling in Engineering and the Environment*. Copyright 2011 Cambridge University Press.[8]

scalar flux, Eq. (24) (thus retaining all production and modeled pressure covariance terms), derived from Eq. (22), can be written as

$$\overline{u_i u_j} = \frac{2}{3}\delta_{ij}k + \frac{k}{\varepsilon}\left[\alpha_1\left(\mathcal{P}_{ij} - \frac{1}{3}\mathcal{P}_{kk}\delta_{ij}\right) + \alpha_2\left(\mathcal{G}_{ij} - \frac{1}{3}\mathcal{G}_{kk}\delta_{ij}\right)\right],$$
(25)

where α_1 and α_2 are functions of $\mathcal{P}_k/\varepsilon$, $\mathcal{G}_k/\varepsilon$ and of the coefficients in the parent modeled differential Eq. (3).

To summarize the position of such truncated versions: if the transport terms are relatively unimportant, as they will often be in flows near walls, or where force fields exert a dominant effect, they may offer a convenient, faster route to a solution that is not significantly different from that of the full second-moment closure. In axisymmetric or three-dimensional free shear flows, however, as noted in Ref.,[74] serious disagreements may arise when stress transport is substantial. As a final such example, Craft et al.[88] using a widely tested, successful NLEVM, found that the scheme predicted a significantly too rapid decay of wing-tip vortices: better than a linear eddy-viscosity model but far less satisfactory than with a full second-moment closure. Clearly, if one seeks to compute flows where a successful track record with such simplified schemes has <u>not</u> been previously established, *emptor caveat*—let the buyer beware!

VII. UNSTEADY RANS (URANS)

There has been a view among some model developers that "pure RANS models can be adjusted to predict boundary layers including separating [flows] well, *but not large separation regions, whether behind a sphere or past buildings, vehicles, in cavities, and so on,*" Spalart.[89] This notion, to some extent conceptual, is however, arguable. It is a position that may correctly reflect experience with simple eddy-viscosity models, but it does not recognize the large variation in the performance of RANS models at different closure levels nor the differences resulting from how individual processes are approximated—topics discussed in earlier sections. There is ample evidence in the literature, some dating back to the mid-1980s (e.g., Celenligil and Mellor[90]) that second-moment closures, with integration up to the wall run in *three-dimensional unsteady mode* (URANS) even for two-dimensional geometries, can return, on a relatively coarse grid, most statistical and even some dynamical features of separated and other complex flows. That is to say, flows which, when viewed overall, may appear steady, nevertheless can be crucially affected by significant "internal unsteadiness" generated by inherent flow instabilities. Such flows do not *necessarily* require a *different kind* of modeling, but rather just an appropriate RANS model run in unsteady mode with a time step sufficiently small to resolve the ensemble-averaged large-scale coherent motion.

The first fully three-dimensional URANS explorations were those of Tatsumi[91] and Kenjereš and Hanjalić.[92] The former examined a backward-facing-step flow using the cubic NLEVM of Craft et al.[93] Kenjereš and Hanjalić[92] applied the URANS strategy via a truncated second-moment approach concept to Rayleigh–Bénard convection in which long-term time averaging results in zero mean velocity, and the fluid motion takes the form of self-organized, unsteady convective roll structures which fill the whole flow domain and provide the mechanism for turbulent heat transport. The approach returned Nusselt numbers and an organized flow topology, both close to the wall and in the bulk region, in accord with LES results obtained with an order-of-magnitude finer grid. Later, the same workers extended the approach to more general cases of thermal convection in different configurations, including the effects of a magnetic field,[94,95] and to both indoor and exterior environmental flows dominated by thermal buoyancy.[84,96]

A recent URANS examination of flow at high Reynolds number over an infinite cylinder in cross flow (often considered a paradigm of massively separated flow), presented in Fig. 12, showed that, in contrast to common eddy-viscosity models, a Reynolds-stress-transport model (RSM) with wall integration captured subtle physical features of the flow including multiple instantaneous separations and reattachments, as well as a low-frequency modulation of the lift and drag coefficient. This behavior was in close accord with LES results obtained on a much finer grid, Palkin et al.[97] This is also true for most of the characteristic features of the "organized" structures: their origin, pattern, size, strength, vorticity intensity, frequency, and amplitude. The success may be attributed to the fact that the stress-transport closure accounts both for the stress anisotropy and the phase lag between the stress and strain eigenvectors. These features resulted in much lower modeled stress and turbulence energy levels than with eddy-viscosity models, Fig. 13 (right) confirming that the stress-transport-closure approach is more sensitive and receptive to internal instabilities. This is further underlined by the resolved turbulence energy level, Fig. 13 (left) being considerably higher than with the eddy viscosity scheme. A further quantitative confirmation of the better resolution of the important large and medium scales by the RSM is provided in Fig. 14 which shows the predicted power spectrum in much closer agreement with the LES than achieved with the EVM.

The accuracy of the computed stochastic field may not be particularly relevant as in such highly separated flows the broadband fluctuations usually do not play a significant role. The main contribution to the total stresses comes from the resolved large-scale, semi-deterministic motions, whether considered as a "mode of mean motion" or coherent turbulent structures. Moreover, a posteriori analysis[95] of the well-resolved LES results for the same flow using a triple decomposition of the velocity into its mean (long-term average), coherent and stochastic components, $U_i = \bar{U}_i + u_i^c + u_i^s$, showed that the "mixed" stress, $u_i^c u_i^s$ is indeed negligible compared with both the coherent ($u_i^c u_i^c$) and stochastic ($u_i^s u_i^s$) constituents, at least for high Reynolds numbers. This confirmed the validity of the (often tacitly hypothesized) scale separation between the coherent and stochastic motion as a prerequisite for the applicability of URANS in flows dominated by such unsteadiness.

It should be acknowledged that even linear eddy-viscosity schemes will sometimes give usefully accurate predictions when run in URANS mode. This is especially so in wall-adjacent flows where the numerical solution extends through the viscosity affected sublayer to the wall (e.g., the study by Basara et al.[98] of the flow past a complete automobile) or where unstable body forces in the *mean* flow equations exert a substantial influence (e.g., results reported in Craft et al.[99] of flow in rotor disk cavities). However, as in the example of flow past a cylinder considered above, the modeled contribution of momentum transport with an EVM is much larger than with a RSM (stress-transport model) while the resolved part is, correspondingly, smaller.

In fact, even with a RSM, the ratio of modeled: resolved stresses is substantially greater than with large-eddy simulation. However, the
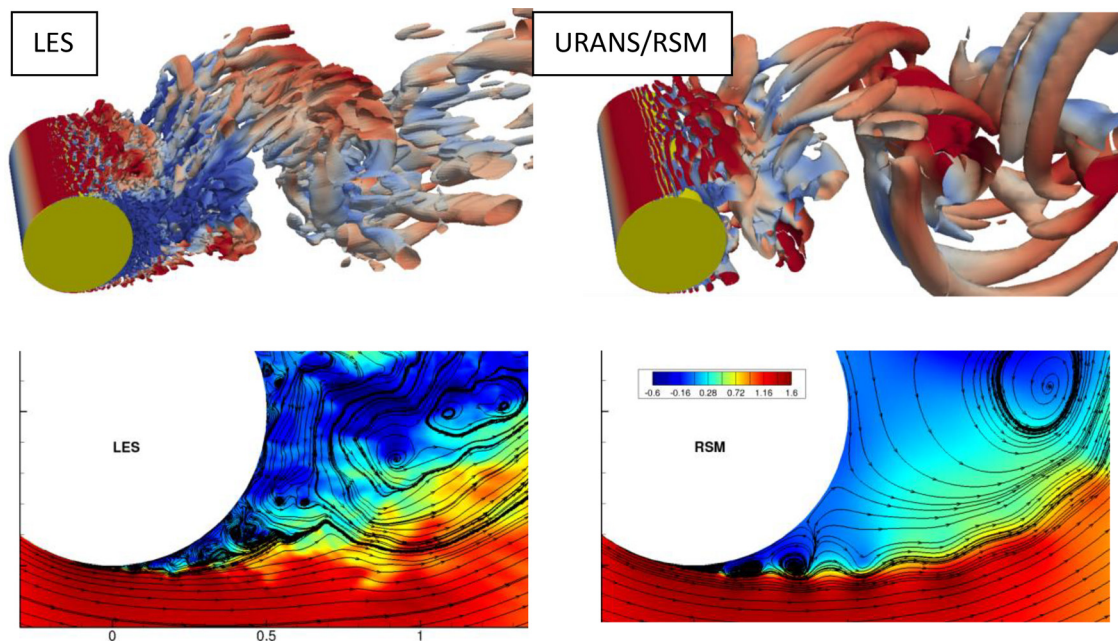
FIG. 12. Flow over an infinite cylinder in the subcritical regime (laminar separation) at Re = 1.4×10^5 Top: comparison of vortical structures (iso-surface of $Q = 0.5$) from LES (post-filtered to the URANS mesh), and URANS RSM, colored with axial velocity. Bottom: a blow-up of the instantaneous near-wall velocity field from LES and RSM at the same phase (based on the lift coefficient). Reproduced with permission from Palkin et al., Flow, Turb. Combust. **97**, 1037 (2016). Copyright 2016 Springer Nature.[97]

forward time step can usually be much larger and the grid density coarser; in consequence, the computational cost to generate a solution with URANS is typically at least an order of magnitude less than for a conventional LES treatment. Moreover, a crucial advantage of URANS in wall-affected flows is its potential to handle flows at very high Reynolds and Rayleigh numbers, which, at present, remain beyond the reach of LES.

As a final example of the power of the URANS approach when employed with a RSM, we consider the off-design flow through a Kaplan turbine examined by Minakov et al.[100] Figure 15 shows the mean flow streamlines in the draft-tube bend. Clearly the RSM computations capture much more closely than the realizable k–ε EVM the

large recirculating vortices present downstream from the impeller predicted by the large-eddy simulation. Further details are provided in Fig. 16 which shows the pair of rotating vortex "ropes" from this test case that were evident in the experiment and well reproduced by the LES. These are also well captured by the RSM computations on a grid of 2×10^6 cells compared with 6×10^6 adopted for the LES. The two-equation eddy-viscosity computations, however, did not generate a time-dependent result on a grid of 2×10^6 cells. Only by refining the mesh to 6×10^6 cells was a time-dependent solution achieved and evidently the predicted pattern both with the "realizable" k–ε version and with the shear-stress transport (SST) k–ω model by no means captures the rope-like structure.
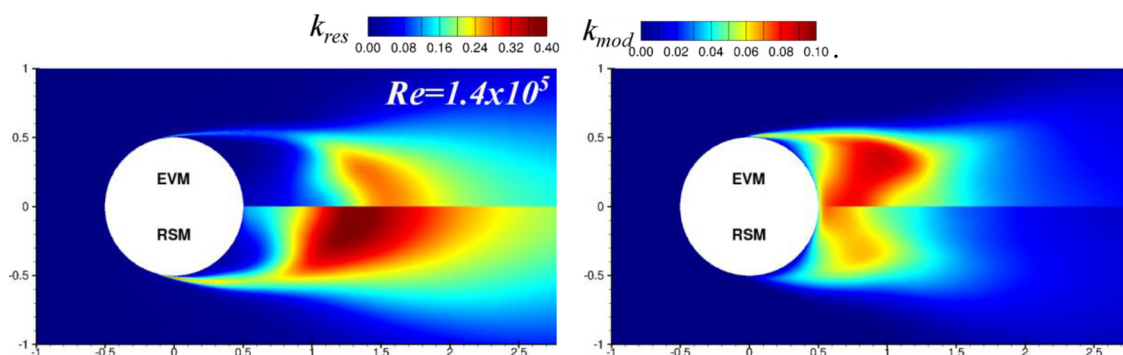

FIG. 13. Flow over an infinite cylinder in subcritical regime at Re = 1.4×10^5. Comparison of the resolved (left) and modeled (right) turbulent kinetic energy from the URANS EVM and RSM models. Reproduced with permission from Palkin et al., Flow Turb. Combust. 97, 1033 (2016). Copyright 2016 Springer Nature.[97]
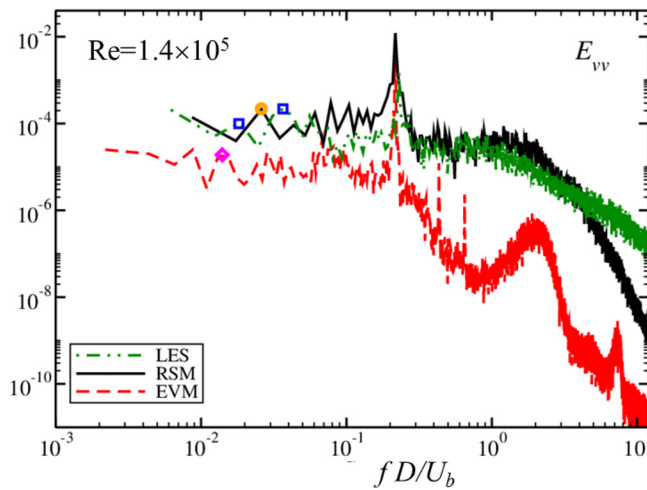
FIG. 14. Flow over an infinite cylinder in subcritical regime at $Re = 1.4 \times 10^5$. Power spectra of flow-normal velocity at $x/D = 0.71$ and $y/D = 0.66$. Reproduced with permission from Palkin *et al.*, Flow Turb. Combust. **97**, 1037 (2016). Copyright 2016 Springer Nature.[97]

VIII. CURRENT TRENDS: HIGHER-ORDER MODELS VERSUS EVMS

The authors have for decades been advocates of using second-moment closure models in the firm belief that, despite their greater demands on computer resources, they captured the physics more faithfully and, thus, should reproduce more accurately complex turbulent flows over a greater range of configurations and conditions than eddy-viscosity schemes. However, the expectation that, with advances in computer hardware, our view would gradually prevail has not in fact come about. Indeed, the opposite has happened: the ever widening of the CFD community and the expansion in the scope of CFD applications has brought about greater demands on CFD-code vendors to ensure their codes' robustness (i.e., certainty to converge to a result), computational economy, and "user friendliness"—demands which inevitably favor simpler models.

Some protagonists of this philosophy have gone so far as to denounce "the relentless attempts to build into them first-principle content and rational ideas" Spalart (This remark was made in the context of limiting the use of RANS models to the wall-adjacent region in hybrid LES-RANS schemes.),[89] arguing that no RANS model can predict flows with massive separation. Industry at large has preferred

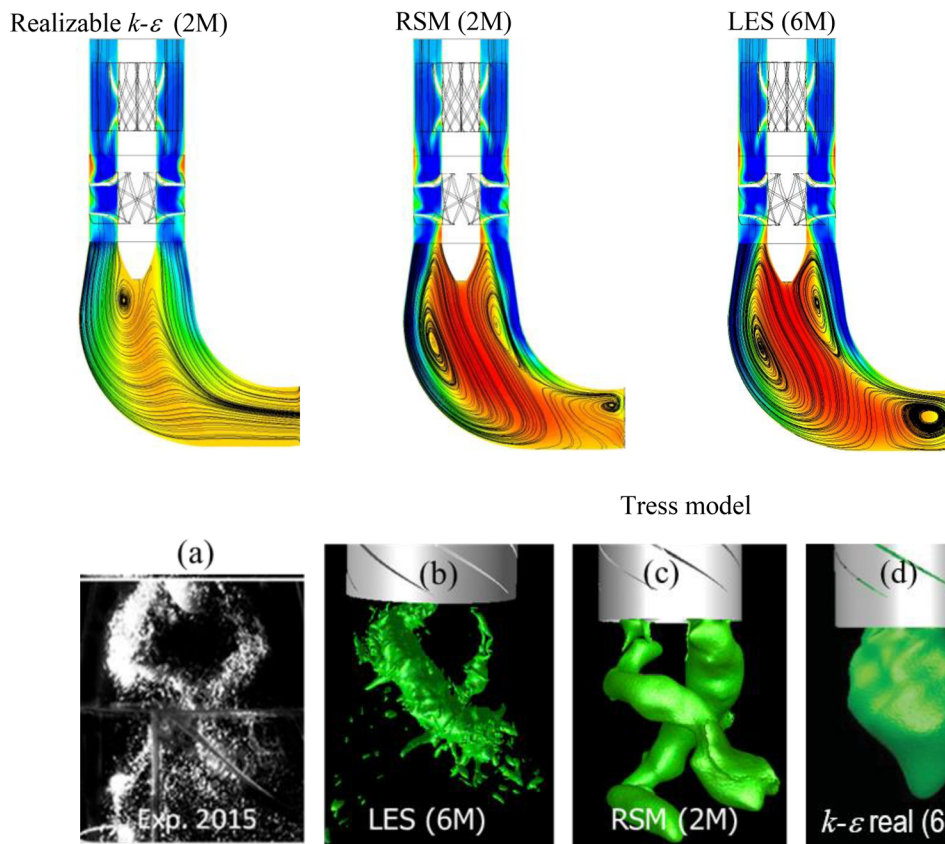Realizable k-ε (2M)   RSM (2M)   LES (6M)

FIG. 15. Time-averaged streamlines colored by axial velocity magnitude (linear color scale from -5.6 m/s, blue, to $+3.0$ m/s, red) in a laboratory model of a Kaplan hydro-turbine in an off-design regime (40% load of the best efficiency point, BEP). Note that the circular cross-section progressively transforms into rectangular at the exit of the draft-tube bend. Comparisons of URANS computations (EVM and RSM) with LES results. Reproduced with permission from Minakov *et al.*, J. Hydraul. Res. **55**, 668 (2017). Copyright 2017 Taylor & Francis Ltd, on behalf of International Association for Hydro-Environment Engineering and Research.

Tress model

FIG. 16. Twin vortex ropes in the draft tube of a laboratory model of a Kaplan hydro-turbine at low load with meshes of 2 M and 6 M cells. (a) Experiment, (b) large-eddy simulation, (c) Reynolds-stress model (second moment closure), and (d) realizable k–ε EVM (e) k–ω SST EVM. Note: the linear EVMs reproduced unsteadiness only on a much finer (6 M) mesh. Reproduced with permission from Minakov *et al.*, J. Hydraul. Res. **55**, 668 (2017). Copyright 2017 Taylor & Francis Ltd, on behalf of International Association for Hydro-Environment Engineering and Research.

simplicity and robustness, even at the expense of physical transparency and comprehensiveness. As a result, CFD software companies have, to a great extent, been responsive to such demands. Some new two-equation and even one-equation eddy-viscosity models have been proposed, tuned for a family of flows particularly suited to certain industrial sectors; indeed, some have become quite popular, despite their containing *ad hoc*, opaque inputs in terms of empirical functions and limiters. One might well conclude that the situation is reminiscent of that of the early days of turbulence modeling a half century ago! Among these, the Spalart-Allmaras (S-A) one-equation model for eddy viscosity (Spalart and Allmaras[101]) and the "shear-stress transport" (SST) k–ω model, Menter[102] are probably the most widely used, at least in the aerospace industry. It seems doubtful that this trend will reverse.

Yet, it *is* recognized that for certain vital applications (whether these be industrial, environmental or medical) *predictive accuracy* still remains of paramount importance. That fact and the increasing geometric complexity of the flow domains to be resolved would seem to favor the employment of second-moment closure. However, even here, the emergence of hybrid LES-RANS approaches (with the RANS region employing an eddy viscosity model) for flows bounded by walls of complex configuration and involving heat and mass transfer offer, for many, the preferred route. So, it may well be the case that differential second-moment closure is destined to remain a relatively minor "niche" market in the firmament of turbulence closure schemes. Nevertheless, there is a reasonable prospect that the better physics embedded in the second-moment approach to closure will, through judicious simplification to algebraic form, still make a significant contribution to enhancing the reliability of CFD for turbulent flows.

DATA AVAILABILITY

Data sharing is not applicable to this article as no new data were created or analyzed in this study.

REFERENCES

[1] O. Reynolds, "On the dynamical theory of incompressible viscous fluids and the determination of the criterion," Philos. Trans. R. Soc. London **186**, 123–164 (1895).

[2] A. Favre, "Equations des gaz turbulents compressibles: Formes générales," J. Méc. **4**, 361–390 (1965).

[3] J. Boussinesq, "Essai sur la théorie des eaux courantes," in *Mémoires Présentés par Divers Savants à l'Académie des Sciences* (Imprimerie Nationale, Paris, 1877), Vol. 23, pp. 1–680.

[4] G. I. Taylor, "Eddy motion in the atmosphere," Philos. Trans. R. Soc. A **215**, 1–25 (1916).

[5] L. Prandtl, "Bericht über untersuchungen zur ausgebildeten turbulenz," ZAMM **5**, 136–139 (1925).

[6] P. R. Spalart, W-H. Jou, M. Strelets, and S. Allmaras "Comments on the feasibility of LES for wings, and on a hybrid RANS/LES approach," in Advances in DNS/LES, edited by C. Liu and Z. Liu (Greyden Press, Columbus, OH, 1997), pp. 137–147.

[7] J. C. Rotta, "Statistische theorie nichthomogener turbulenz," Z. Phys. **129**, 547–572 (1951).

[8] K. Hanjalić and B. E. Launder, *Turbulence Modelling in Engineering and the Environment*, 2nd ed. (Cambridge University Press, 2021).

[9] M. D. Millionshtchikov, "On the theory of homogeneous isotropic turbulence," C. R. Acad. Sci. SSSR **32**, 615–619 (1941).

[10] P. Y. Chou, "On the velocity correlations and the solutions of the equations of turbulent fluctuations," Q. J. Appl. Math. **3**, 38–54 (1945).

[11] J. C. André, G. de Moor, P. Lacarrère, G. Thierry, R. du Vachat, "The clipping approximation and inhomogeneous turbulence simulations," in *Turbulent Shear Flows 1*, edited by F. J. Durst *et al.* (Springer Verlag, Heidelberg, 1979), pp. 307–318.

[12] T. J. Craft, J. Kidger, and B. E. Launder, "Importance of 3rd-moment modelling in horizontal, stably stratified flow," *Proceedings of 11th Symposium on Turbulent Shear Flows*, Grenoble, France, 8-10 September, 1997, pp. 20.13–20.18.

[13] D. Naot, A. Shavit, and M. Wolfshtein, "Interactions between components of the turbulent correlation tensor," Isr. J. Technol. **8**, 259–269 (1970).

[14] B. E. Launder, "On the effects of a gravitational field on the turbulent transport of heat and momentum," J. Fluid Mech. **67**, 569–581 (1975).

[15] U. Schumann, "Numerical simulation of the transition from three- to two-dimensional turbulence under a uniform magnetic field," J. Fluid Mech. **74**, 31–58 (1976).

[16] S. Kenjeres, K. Hanjalić, and D. Bal, "A DNS-based second-moment closure for turbulent magnetohydrodynamic flows," Phys. Fluids **16**, 1229–1241 (2004).

[17] S. C. Crow, "Visco-elastic properties of fine-grained incompressible turbulence," J. Fluid Mech. **33**, 1–20 (1968).

[18] W. P. Jones and A. Manners, "The calculation of the flow through a two-dimensional faired diffuser," in *Turbulent Shear Flows*, edited by J. C. André *et al.* (Springer Verlag, Heidelberg, 1989), Vol. 6, pp. 18–31.

[19] S. J. Stevens and P. Fry, "Measurement of the boundary layer growth in annular diffusers," J. Aircraft **10**, 73–80 (1973).

[20] K. Hanjalić and B. E. Launder, "Fully developed asymmetric flow in a plane channel," J. Fluid Mech. **51**, 301–335 (1972).

[21] K. Hanjalić and B. E. Launder, "A Reynolds stress model of turbulence and its application to thin shear flows," J. Fluid Mech. **52**, 609–638 (1972).

[22] B. J. Daly and F. H. Harlow, "Transport equations in turbulence," Phys. Fluids **13**, 2634–2649 (1970).

[23] D. Naot, A. Shavit, and M. Wolfshtein, "Two-point correlation model and the redistribution of Reynolds stress," Phys. Fluids **16**, 738 (1973).

[24] U. Schumann, "Realizability of Reynolds-stress turbulence models," Phys. Fluids **20**, 721–725 (1977).

[25] J. L. Lumley, "Computational modeling of turbulent flows," Adv. Appl. Mech. **18**, 123–176 (1978).

[26]T.-H. Shih and J. L. Lumley, "Modeling of pressure correlation terms in Reynolds stress and scalar flux equations," Report No. FDA-85-3, Sibley School of Mechanical & Aerospace Engineering, Cornell University, Ithaca, NY, 1985.

[27]S. Fu, "Computational modelling of turbulent swirling flows with second-moment closures," Ph.D. thesis (Faculty of Engineering, University of Manchester, 1988).

[28]T. J. Craft and B. E. Launder, "Closure modelling near the two-component limit," in Closure Strategies for Turbulent and Transitional Flows, edited by B. E. Launder and N. D. Sandham (Cambridge University Press, 2002).

[29]T. J. Craft and B. E. Launder, "On the spreading mechanism of the three-dimensional turbulent wall jet," J. Fluid Mech. **435**, 305–326 (2001).

[30]B. E. Launder and S.-P. Li, "On the elimination of wall-topography parameters from second-moment closure," Phys. Fluids **6**, 999–1006 (1994).

[31]J. O. Hinze, "Experimental investigation on secondary currents in turbulent flow through a straight conduit," Appl. Sci. Res. **28**, 453–465 (1973).

[32]C. Speziale, S. Sarkar, and T. B. Gatski, "Modelling the pressure-strain correlation: An invariant dynamical systems approach," J. Fluid Mech. **227**, 245–272 (1991).

[33]P. Durbin, "Near-wall turbulence closure modelling without damping functions," Theor. Comput. Fluid Dyn. **3**, 1–13 (1991).

[34]S. B. Pope, "An explanation of the round-jet/plane-jet anomaly," AIAA J. **16**, 3311–3340 (1978).

[35]K. Hanjalić and B. E. Launder, "Sensitizing the dissipation equation to secondary strains," ASME J. Fluids Eng. **102**, 34–40 (1980).

[36]T. J. Craft and B. E. Launder, "A Reynolds-stress closure designed for complex geometries," Int. J. Heat Fluid Flow **17**, 245–254 (1996).

[37]K. Hanjalić, "Some resolved and unresolved issues in modelling non-equilibrium and unsteady turbulent flows," in Engineering Turbulence Modelling and Measurements -3, edited by W. Rodi and G. Bergeles (Elsevier, Amsterdam, 1996), pp. 3–18.

[38]H. Iacovides and M. Raisee, "Recent progress in the computation of flow and heat transfer in internal cooling passages of gas turbines," Int J. Heat Fluid Flow **20**, 320–328 (1999).

[39]D. C. Wilcox, "Reassessment of the scale-determining equation for advanced turbulence models," AIAA J. **26**, 1311–1320 (1988).

[40]D. C. Wilcox, Turbulence Modeling for CFD, 2nd ed. (DCW Industries, La Cañada, CA, 2000).

[41]K. Hanjalić and B. E. Launder, "Contribution towards a Reynolds-stress closure for low-Reynolds-number turbulence," J. Fluid Mech. **74**, 593–610 (1976).

[42]B. E. Launder and D. P. Tselipidakis, "Application of a new second-moment closure to turbulent channel flow rotating in orthogonal mode," Int. J. Heat Fluid Flow **15**, 2–10 (1994).

[43]K. Hanjalić and S. Jakirlić, "Second-moment turbulence closure modelling," in Closure Strategies for Laminar and Turbulent Flows, edited by B. E. launder and N. D. Sandham (Cambridge University Press, Cambridge, 2002), 47–101.

[44]S. Hoyas and J. Jimenez, "Scaling of velocity fluctuations in turbulent channels up to $\mathcal{R}e_\tau = 2003$," Phys. Fluids **18**, 0011702 (2006).

[45]K. Hanjalić and S. Jakirlić, "A model of stress dissipation in second-moment closures," Appl. Sci. Res. **51**, 513–518 (1993).

[46]K. Hanjalić, S. Jakirlić, I. Hadžić, "Computation of oscillating turbulent flows at transitional re-numbers," Turbulent Shear Flows-9, edited by F. J. Durst et al. (Springer Verlag, Berlin, 1995), pp. 323–342.

[47]K. Hanjalić and S. Jakirlić, "Contribution towards the second-moment closure modelling of separating turbulent Flows," Comput. Fluids **27**(2), 137–156 (1998).

[48]S. Jakirlić, K. Hanjalić, and C. Tropea, "Modeling rotating and swirling turbulent flows: A perpetual challenge," AIAA J. **40**(10), 1984–1996 (2002).

[49]J. Jovanović, Q. Y. Ye, and F. Durst, "Statistical interpretation of the turbulent dissipation rate in wall-bounded flows," J. Fluid Mech. **293**, 321–457 (1995).

[50]S. Jakirlić and K. Hanjalić, "A new approach to modelling near-wall turbulence energy and stress dissipation," J. Fluid Mech. **459**, 139–166 (2002).

[51]P. A. Durbin, "A Reynolds stress model for near-wall turbulence," J. Fluid Mech. **249**, 465–498 (1993).

[52]V. Wizman, D. Laurence, M. Kanniche, P. Durbin, and A. Demuren, "Modeling near-wall effects in second-moment closure by elliptic relaxation," Int. J. Heat Fluid Flow **17**, 255–266 (1996).

[53]R. Manceau and K. Hanjalić, "A new form of the elliptic relaxation equation to account for wall effects in RANS modelling," Phys. Fluids **12**, 2345–2351 (2000).

[54]R. Manceau, M. Wang, and D. Laurence, "Inhomogeneity and anisotropy effects on the redistribution terms in RANS modelling," J. Fluid Mech. **438**, 307–338 (2001).

[55]R. Manceau and K. Hanjalić, "The elliptic blending model: A new near-wall Reynolds-stress closure," Phys. Fluids **14**, 744–754 (2002).

[56]R. Manceau, "An improved version of the elliptic blending model: Application to non-rotating and rotating channel flows," Proceeding of 4th International Symposium on Turbulence & Shear Flow Phenomena, edited by J. A. C. Humphrey et al. , Williamsburg, VA, 27-29 June 2005, pp. 259–264.

[57]O. Lamballais, O. Métais, and M. Lesieur, "Spectral dynamic model for large-eddy simulation of rotating channel flow," Theor. Comput. Fluid Dyn. **12**, 149–177 (1998).

[58]W. P. Jones and P. Musonge, "Closure of the Reynolds stress and scalar flux equation," Phys. Fluids **31**, 3589–3604 (1988).

[59]S. Corrsin, "Heat transfer in isotropic turbulence," J. Appl. Phys. **23**, 113–118 (1952).

[60]C. Donaldson, P. du, R. D. Sullivan, and H. Rosenbaum, "A theoretical study of the generation of atmospheric clear-air turbulence," AIAA J. **10**, 162–170 (1972).

[61]J. L. Lumley, "A model for computation of stratified turbulent flows," in International Symposium on Stratified Flows, Novosibirsk, Russia (1972).

[62]C. A. G. Webster, "An experimental study of turbulence in a density stratified shear flow," J. Fluid Mech. **19**, 221–245 (1964).

[63]T. J. Craft, A. V. Gerasimov, H. Iacovides, and B. E. Launder, "The negatively buoyant turbulent wall jet: Performance of alternative options in RANS modelling," Int. J. Heat Fluid Flow **25**, 809–823 (2004).

[64]T. J. Craft and B. E. Launder, "Application of TCL modelling to stratified flows," in Closure Strategies for Turbulent and Transitional Flows, edited by B. E. Launder and N. D. Sandham (Cambridge University Press, Cambridge, 2002), Chap. 14, pp. 407–423.

[65]Y. Adad, S. Benhamadouche, and D. Laurence, "The negatively buoyant wall jet: The LES results," Int. J. Heat Fluid Flow **25**, 795–808 (2004).

[66]C. D. Donaldson, "Atmospheric turbulence and the dispersal of atmospheric pollutants," in Proceedings of Workshop on Micrometeorology, edited by D. A. Haugen (American Meteorological Society, Science Press, 1973), pp. 313–390.

[67]G. M. Mellor and T. Yamada, "A hierarchy of turbulence closure models for planetary boundary layers," J. Atmos. Sci. **31**, 1791–1806 (1974).

[68]J. C. Wyngaard, "Modeling the planetary boundary layer-extension to the stable case," Boundary-Layer Meteorol. **9**, 441–460 (1975).

[69]W. S. Lewellen, M. E. Teske, and C. D. P. Donaldson, "Variable density flows computed by a second-order closure description of turbulence," AIAA J. **14**(3), 382–387 (1976).

[70]G. L. Mellor and T. Yamada, "Development of a turbulence closure model for geophysical fluid problems," Rev. Geophys. Space Phys. **20**(4), 851–875, https://doi.org/10.1029/RG020i004p00851 (1982).

[71]H. S. Dol, K. Hanjalić, and S. Kenjereš, "A comparative assessment of the second-moment differential and algebraic models in turbulent natural convection," Int. J. Heat Fluid Flow **18**, 4–14 (1997).

[72]K. Hanjalić, "One-point closure models for buoyancy-driven turbulent flows," Ann. Rev. Fluid Mech. **34**, 321–347 (2002).

[73]L. Umlauf and H. Burchard, "A generic length-scale equation for geophysical turbulence models," J. Mar. Res. **61**, 235–265 (2003).

[74]W. Rodi, "Examples of calculation methods for flow and mixing in stratified fluids," J. Geophys. Res. **92**, 5305–5328, https://doi.org/10.1029/JC092iC05p05305 (1987).

[75]W. Rodi, "The prediction of free turbulent boundary layers by use of a 2-equation model of turbulence," Ph.D. thesis (University of London, 1972).

[76]W. Rodi and G. Scheuerer, "Calculation of curved shear layers with 2-equation turbulence models," Phys. Fluids **26**, 1422–1436 (1983).

[77]B. E. Launder and W. M. Ying, "Prediction of flow and heat transfer in ducts of square cross-section," Proc. Inst. Mech. Eng. **187**, 455–461 (1973).

[78]S. Fu, B. E. Launder, and M. A. Leschziner, "A comparison of algebraic and differential second-moment closures for axisymmetric free shear flows," J. Fluids Eng. **110**, 216–221 (1988).

[79]S. B. Pope, "A more general effective eddy viscosity hypothesis," J. Fluid Mech. **72**, 331–340 (1975).

[80]T. B. Gatski and C. G. Speziale, "On explicit algebraic stress models for complex turbulent flows," J. Fluid Mech. **254**, 59–78 (1993).

[81]S. Wolfram, *MathematicaTM* (Addison Wesley, Boston, 1988).

[82]T. B. Gatski and C. L. Rumsey, "Linear and non-linear eddy viscosity models," in *Closure Strategies for Turbulent and Transitional Flows*, edited by B. E. Launder and N. D. Sandham (Cambridge University Press, 2002).

[83]S. Wallin and S. V. Johansson, "An explicit Reynolds stress model for incompressible and compressible turbulent flows," J. Fluid Mech. **403**, 89–132 (2000).

[84]S. Kenjereš and K. Hanjalić, "Tackling complex turbulent flows with transient RANS," Fluid Dyn. Res. **41**, 012201 (2009).

[85]H. Schmidt and U. Schumann, "Coherent structure of the convective boundary layer derived from Lare-eddy simulations," J. Fluid Mech. **200**, 511–562 (1989).

[86]J. W. Deardorff, G. E. Willis, and D. K. Lilly, "Laboratory investigation of non-steady penetrative convection," J. Fluid Mech. **35**, 7–31 (1969).

[87]O. Zeman and J. L. Lumley, "Modeling buoyancy driven mixed layers," J. Atmos. Sci. **33**, 1974–1988 (1976).

[88]T. J. Craft, A. V. Gerasimov, B. E. Launder, and C. M. Robinson, "A computational study of the near-field generation and decay of wingtip vortices," Int. J. Heat Fluid Flow **27**, 684–695 (2006).

[89]P. R. Spalart, "Detached-eddy Simulation," Ann. Rev. Fluid Mech. **41**, 181–202 (2009).

[90]M. C. Celenligil and G. L. Mellor, "Numerical solution of two-dimensional turbulent separated flows using a Reynolds stress closure," J. Fluids Eng. **107**, 467–476 (1985).

[91]K. Tatsumi, H. Iwai, E. C. Neo, K. Inaoka, and K. Suzuki, "Prediction of time-mean characteristics and periodical fluctuation of velocity and thermal fields of a backward-facing step, 1167–1172," *Turbulence & Shear-Flow Phenomena*, edited by S. Banerjee and J. K. Eaton (Begell House, New York, 1999), Vol. 1.

[92]S. Kenjereš and K. Hanjalić, "Transient analysis of Rayleigh-Bénard convection with a RANS model," Int. J. Heat Fluid Flow **20**, 329–340 (1999).

[93]T. J. Craft, B. E. Launder, and K. Suga, "Development and application of a cubic eddy-viscosity model of turbulence," Int. J. Heat Fluid Flow **17**, 108–115 (1996).

[94]K. Hanjalić and S. Kenjereš, "T-RANS' simulation of deterministic eddy structure in flows driven by thermal buoyancy and Lorentz force," Flow, Turb. Combust. **66**, 427–451 (2001).

[95]S. Kenjereš and K. Hanjalić, "Numerical simulation of a turbulent magnetic dynamo," Phys. Rev. Lett. **98**, 104501 (2007).

[96]M. Hrebtov and K. Hanjalić, "Numerical study of winter diurnal convection over the city of Krasnoyarsk: Effects of non-freezing river, undulating fog and steam devils," Boundary Layer Meteorol. **163**, 469–495 (2017).

[97]E. Palkin, R. Mullyadzhanov, M. Hadžiabdć, and K. Hanjalić, "Scrutinizing URANS in shedding flows: The case of cylinder in cross-flow in the subcritical regime," Flow Turb. Combust. **97**, 1017–1046 (2016).

[98]B. Basara, F. M. Aldudak, M. Schrefl, S. Jakirlić, K. Hanjalić, C. Tropea, and J. Mayer, "Experimental investigations and computations of unsteady flow past a real car using a robust elliptic relaxation closure with a universal wall treatment," in *SAE Paper 2007-01-0104*, *SAE World Congress*, Detroit, MI, April 16, 2007.

[99]T. J. Craft, H. Iacovides, B. E. Launder, and A. Zacharos, "Some swirling-flow challenges for turbulent CFD," Flow, Turb. Combust. **80**, 419–434 (2008).

[100]A. V. Minakov, D. V. Platonov, I. V. Litvinov, S. I. Sergey I. Shtork, and K. Hanjalić, "Vortex ropes in draft tube of a laboratory Kaplan hydroturbine at low load: An experimental and LES scrutiny of RANS and DES computational models," J. Hydraul. Res. **55**(5), 668–685 (2017).

[101]P. R. Spalart and S. R. Allmaras, "A one-equation turbulence model for aerodynamic flows," AIAA Paper No. 92-0439, 1992.

[102]F. R. Menter, "Two-equation eddy-viscosity model for engineering applications," AIAA J. **32**, 1598–1605 (1994).